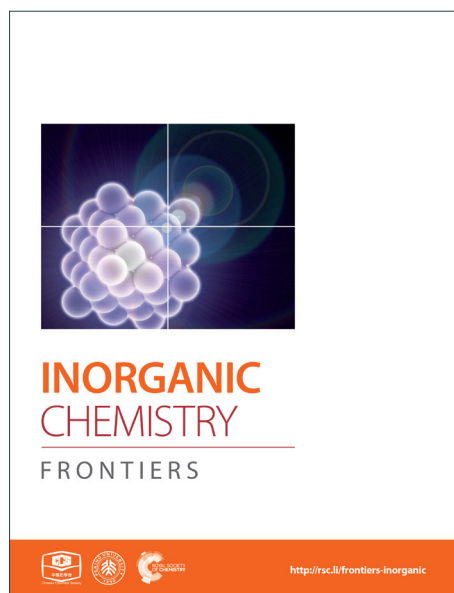
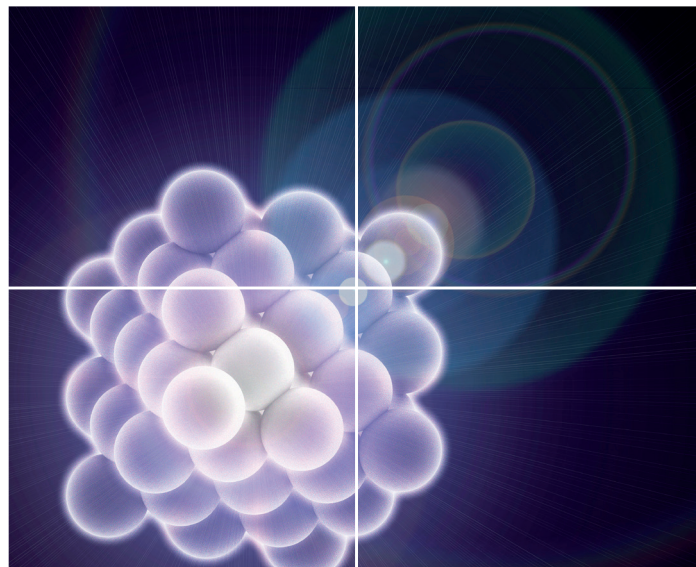


INORGANIC CHEMISTRY

FRONTIERS

Accepted Manuscript



This is an *Accepted Manuscript*, which has been through the Royal Society of Chemistry peer review process and has been accepted for publication.

Accepted Manuscripts are published online shortly after acceptance, before technical editing, formatting and proof reading. Using this free service, authors can make their results available to the community, in citable form, before we publish the edited article. We will replace this *Accepted Manuscript* with the edited and formatted *Advance Article* as soon as it is available.

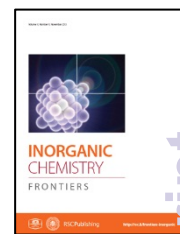
You can find more information about *Accepted Manuscripts* in the [Information for Authors](#).

Please note that technical editing may introduce minor changes to the text and/or graphics, which may alter content. The journal's standard [Terms & Conditions](#) and the [Ethical guidelines](#) still apply. In no event shall the Royal Society of Chemistry be held responsible for any errors or omissions in this *Accepted Manuscript* or any consequences arising from the use of any information it contains.



Frontiers is a unique collaboration between the Chinese Chemical Society and the Royal Society of Chemistry, aiming to publish a series of high impact quality chemistry journals that showcase the very best research from China, Asia and the rest of the world to an international audience. Each journal title is launched in collaboration with a top Chinese institute in the relevant field. For *Inorganic Chemistry Frontiers*, this is Peking University.

<http://rsc.li/frontiers-inorganic>



Guidelines for Referees - Communication Submission

Inorganic Chemistry Frontiers is a high impact Journal publishing research into inorganic and organometallic molecules and solids with explicit applications. This includes inorganic chemistry research at the interfaces of materials science, energy, nanoscience, catalysis and bio-inorganic chemistry. Papers should be of high significance and answer fundamental questions relevant to interdisciplinary applications.

Preliminary accounts of original and significant work of such importance that rapid publication is justified may be published in Communication form. Communications that do not meet the requirement for urgent publication may be invited as full-paper re-submissions. The recommended length for a communication is four journal pages, however some flexibility is allowed.

Thank you very much for your assistance in evaluating this manuscript.

Best wishes

So GAO, 高松

Song GAO, 高松, Peking University

Editor-in-Chief, *Inorganic Chemistry Frontiers*, InorgChemFrontiersED@rsc.org

General Guidance - Please be aware of our [Ethical Guidelines](#), which contain full information on the responsibilities of referees and authors, and our [Refereeing Procedure and Policy](#).

When preparing your report, please:

- Comment on the originality, significance, impact and scientific reliability of the work;
- State clearly whether you would like to see the article accepted or rejected and give detailed comments (with references, as appropriate) that will both help the Editor to make a decision on the article and the authors to improve it.

For confidentiality reasons, please:

- Treat the work and the report you prepare as confidential; the work may not be retained (in any form), disclosed, used or cited prior to publication; if you need to consult colleagues to help with the review, please inform them that the manuscript is confidential, and inform the Editor;
- Do not communicate directly with authors; *NB* your anonymity as a referee will be strictly preserved from the authors.

Please inform the Editor if:

- There is a conflict of interest;
- There is a significant part of the work which you are not able to referee with confidence;
- The work, or a significant part of the work, has previously been published or is currently submitted elsewhere;
- The work represents part of an unduly fragmented investigation.

When submitting your report, please:

- Provide your report rapidly and within **ten days**, or inform the Editor immediately if you cannot do so. We welcome suggestions of alternative referees.

If you have any questions about reviewing this manuscript, please contact InorgChemFrontiersPROD@rsc.org

Submit your report at <http://mc.manuscriptcentral.com/inorgcf>

Justification

- 1 Ultrasmall and monodisperse air-stable colloidal Nd-Fe-B nanoparticles (NPs) have been synthesized by solution phase colloidal method.
- 2 The critical temperature (T_C) of Nd-Fe-B nanoparticle with 3 nm in diameter is surprisingly high, higher than 650 K.
- 3 The size of them can be controlled in the sub-5-nm regime.
- 4 EXAFS gives the chemical environmental information of the Fe center and Mössbauer spectroscopy confirms the 3 nm Nd-Fe-B nanoparticle containing the Fe nanocluster.
- 5 The possible magnetic coupling mechanism is proposed.

From: Prof. Dr. Bing Yan
Department of Chemistry,
Tongji University,
Siping Road 1239,
Shanghai, 200092
People's Republic of China
Fax: +86-21-65982287
Tel: +86-21-65984663
E-mail: byan@tongji.edu.cn

To: Editorial Office,
Inorganic Chemistry Frontiers

April 6th, 2014

Dear Editor,

We would like to resubmit one electronically original manuscript as a communication (previous submission No. QI-COM-01-2014-000002) entitled "Ultrasmall and monodisperse colloidal amorphous Nd-Fe-B-Na magnetic nanoparticles with high T_C " to Inorganic Chemistry Frontiers. The authors are Qiang Zhang, Zheng Jiang and Bing Yan*. The whole manuscript contains 4 pages including the title, authors, address, abstract, text, references and five figures together with another 9 pages of supplementary information pages. Monodisperse colloidal magnetic nanoparticles, such as ϵ -Co, FePt, CoFe₂O₄, and Fe₃O₄, have been synthesized and characterized. However, the blocking temperatures (T_B) of the above mentioned nanomagnets with about 5 nm diameter based on long-range ferromagnetic interactions are far below room temperature, although the magnetocrystalline anisotropy of their bulk crystalline phase are large. Short-range order structure and random magnetic anisotropy of ferromagnetic amorphous phase RE-TM and RE-TM-B alloys (RE = rare-earth metal, TM = transition metals) with high T_C inspire us that the undesirable affect of decreasing size on T_C is not like that of crystalline phase. In this paper, we report colloidal synthesis and magnetic properties of air-stable monodisperse amorphous Nd-Fe-B-Na nanoparticle with 3 nm in diameter and T_C higher than 650 K. We have revised the manuscript according to the referees' comments of the previous submission No. QI-COM-01-2014-000002. The detailed revision has been shown in the attached pages and the revision details are marked in yellow face. We would like to look forward to seeing this paper can be accepted for published in Inorganic Chemistry Frontiers.

Sincerely yours,

Bing Yan

Response to the comments for our previous submission No. QI-COM-01-2014-000002) entitled "Ultrasmall and monodisperse colloidal amorphous Nd-Fe-B-Na magnetic nanoparticles with high T_c " to Inorganic Chemistry Frontiers by Qiang Zhang, Zheng Jiang and Bing Yan*.

Reviewer(s)' Comments to Author:

Referee: 1

Rating: Routine (top 25-50%)

Comments to the Author

Magnetic nanoparticles (NPs) have attracted intensive research in the past decades due to their potential applications in high-density magnetic recording media and nanocomposite permanent magnets. This manuscript presents a study on the structural and magnetic properties of the ultrasmall Nd-Fe-B-Na nanoparticles (NPs) prepared by a solution phase colloidal method. Based on the x-ray absorption fine structure (XAFS) and Mössbauer spectrum analyses, the authors considered that the observed high-temperature ferromagnetism was attributed to the Fe nanocluster. However, the present results could not sufficiently support the conclusions about the origin of the observed high-temperature ferromagnetism. Therefore, I cannot recommend the publication of this manuscript. After revision, the manuscript might be suitable for another journal. Here are several questions and suggestions to improve the presentation and justify some of the main findings, primarily focusing on providing a better context of this work and explaining the nature of the reported magnetic ordering.

Response: We are appreciated to the reviewer's comments and evaluation. We should have made it clearer that the observed high-temperature ferromagnetism was attributed to the amorphous phase, as shown in Figure 1a red curve. The ferromagnetism of Fe nanocluster was also attributed to their surrounding amorphous phase, because Fe nanoparticles usually exhibit superparamagnetism at room temperature as soon as the particle size reduced to several nanometers. But, the ferromagnetism of Fe nanocluster could inversely enhance high-temperature ferromagnetism.

1. On the basis of the XAFS and Mössbauer spectrum results, the authors considered that the high-temperature ferromagnetism in Nd-Fe-B-Na nanoparticle with 3 nm was attributed to the Fe

nanocluster included in the nanoparticles. As is known, the ferromagnetic metal nanoparticles, such as Co and Fe, etc., usually exhibit superparamagnetism as the particle size reduced to several nanometers. Therefore, it is necessary to elucidate how the superparamagnetic limit is broken via the interactions between the Fe nanocluster and the amorphous materials.

Response: We are appreciated to the reviewer's comments and concern. From the ^{57}Fe Mössbauer spectrum, there are two kinds of Fe nuclei in blocked states. So, the observed high-temperature ferromagnetism was attributed to both the amorphous phase and the Fe nanocluster for the 3 nm Nd-Fe-B-Na nanoparticles. It is necessary and highly interesting to elucidate how the superparamagnetic limit is broken *via* the interface interactions between the Fe nanocluster and the amorphous surrounding materials. But, the initial and major target of this paper is on colloidal synthesis and magnetic characterizations and we think that it will be our future work. Thank you very much for your valuable comment.

2. It is shown that the ^{57}Fe Mössbauer spectrum of the Nd-Fe-B-Na nanoparticles was changed significantly along with the increase of the particle size (doublet and sextet subspectra appeared in order). The authors should clarify the nature underlying these spectral changes.

Response: We are appreciated to the reviewer's comments. Doublet subspectra means the Fe nuclei in paramagnetic states, while sextet subspectra means the Fe nuclei in blocked states. Along with the increase of the particle size, there are more Fe nuclei in blocked states.

3. The authors considered that there are two different atomic-structured Fe ions in Nd-Fe-B-Na nanoparticles. This case should be taken into account in the process of XAFS fitting. The present fitting results did not reflect the presence of Fe nanocluster. Moreover, the fitting curves should be included in the text.

Response: We are appreciated to the reviewer's comments. For XAFS fitting, they are based on the metal atoms (majorly on the atomic number, Z) and their coordinating environments at near 1 nm space scale, including the coordinating number, configuration, and nature of the coordinating atoms. So, it's not technical viable to take into account the different chemical valance of the Fe ions. Under current fitting model, the peaks at 2.58 Å, 3.9 Å, and 4.6 Å in Figure 3 in the main text shows the presence Fe nanoclusters. The major magnitude is from the Fe in the amorphous phase.

4. It is clear that there are two distinct local structures of Fe ions in the Nd-Fe-B-Na nanoparticles, i.e., one in Fe nanocluster and the other one in amorphous Nd-Fe-B-Na alloy. The authors should use their XPS results to discuss whether there are valence differences between these two kinds of Fe ions.

Response: We are appreciated to the reviewer's comments. XPS is powerful to discover the difference between Fe⁽⁰⁾ and Fe^(II) or Fe^(III). But, the XPS is based on the surface information, but the Fe⁽⁰⁾ nanoclusters are buried inside the amorphous phase. We have done the XPS measurement shown in Figure S3, but did not find the peak corresponding Fe⁽⁰⁾ at 2p_{3/2} at 706.6 eV. (See Figure S3 in ESI)

5. As the particle size of Nd-Fe-B-Na nanoparticles increases from 3 to 5 nm, the shapes of the hysteresis loops are changed obviously. The authors should give some quantitative explanations.

Response: We are appreciated to the reviewer's comments. We are also interested in the difference between the shapes of the hysteresis loops of 3 to 5 nm Nd-Fe-B-Na nanoparticles. At present, we attribute this to the different measurement facilities, SQUID-VSM for the 3 nm Nd-Fe-B-Na nanoparticles and a LakeShore 7407 vibrating sample magnetometer (VSM) for the 5 nm Nd-Fe-B-Na nanoparticles. We have noted this by yellow face words in the caption of Figure S7 at the ESI of this paper. (See Figure S7 in ESI)

Referee: 2

Rating: Significant (top 10-25%)

Comments to the Author

In this article, authors synthesized amorphous Nd-Fe-B-Na nanoparticles with different particle size. Besides, when the particle size is 3 nm, it suggests ferromagnetic property and has a higher T_c, but the magnetic property is too low compare with crystalline nanocomposite. The authors also take advantage of some kinds of measurement techniques to prove the mechanism.

Having critical reading of the manuscript it is suggested to address the following observations as major revision.

Response: We are appreciated to the reviewer's comments and evaluation.

1. One suggestion for the TEM characterizations, you'd better to give the same resolution (scale bar), it will be easy for readers to understand the difference of particle size.

Response: We are appreciated to the reviewer's comments. Your suggestion is nice, but for our TEM images, the present ones are clearer

2. Supporting information: The EDS data, you found a strong peak belong to Si and O, you mentioned it maybe come from SiO₂ contaminant, so where is the SiO₂ contaminant come from? Can you refine it? Besides, "Considering the intrinsic oxophilic properties of Nd^(III) and the presence of water and other oxygen-containing molecular species, the Nd-Fe-B-Na nanoparticles could contain some oxygen." In this sentence, you also mentioned the existent of oxygen. So it will be confusing for audience.

Response: We are appreciated to the reviewer's comments. We are adopting a JEOL JEM-2010F electron microscope equipped with an older detector, so we get a small silicon internal fluorescence peak from Si dead layer of Si-Li detector. This is even more significant when the number and volume of the Nd-Fe-B-Na nanoparticles are small which determines the intensity of the sample.

3. You'd better to simply explain why the magnetic property decreasing after exposing to air several day.

Response: We are appreciated to the reviewer's comments. The colloidal the Nd-Fe-B-Na nanoparticles are synthesized in a reducing environment dictated by the presence of borides. So, the chemical valence of Fe are not all in the stable states, which are supported by the presence of Fe⁽⁰⁾ nanocluster. The magnetic property decreasing after exposing to air are due to the oxidation of the trace surface unstable Fe (e.g., Fe^(I) or Fe^(II)) or Fe⁽⁰⁾ nanocluster. We add this to the main text and label as yellow face. (See the bottom of page 2)

If above points are clarified the manuscript may be accepted for publication

You also have to add more references: J. Mater. Chem. C 2013, 1, 275 and J. Nanosci. Nanotech. 2013, 13, 7717.

Response: We are appreciated to the reviewer's comments and evaluation. These two papers are important on the combination of the sol-gel method and high temperature reduction method one the

synthesis of Nd-Fe-B nanomaterials and nanocomposites. Our method is based on colloidal synthesis, involving organic surfactants, molecular precursors, nucleation and growth at the organic and inorganic interface, which are totally different with the sol-gel method and high temperature reduction method in mechanism. This is the reason why we cited papers on colloidal methods to get freestanding magnetic nanoparticles. According to the comment, we have added the citation of the two references in the introduction section. (See ref.9b,9c)

COMMUNICATION

Ultrasmall and monodisperse colloidal amorphous Nd-Fe-B-Na magnetic nanoparticles with high T_C

Cite this: DOI: 10.1039/x0xx00000x

Q. Zhang^a, Z. Jiang^b and B. Yan^a

Received 00th January 2012,

Accepted 00th January 2012

DOI: 10.1039/x0xx00000x

www.rsc.org/

Abstract Ultrasmall and monodisperse air-stable colloidal Nd-Fe-B-Na nanoparticles (NPs) have been synthesized by solution phase colloidal method and characterized by TEM, EXAFS, Mössbauer spectroscopy, and SQUID. The size of them can be controlled in the sub-5-nm regime. The critical temperature (T_C) of Nd-Fe-B-Na nanoparticle with 3 nm in diameter is surprisingly high, higher than 650 K. EXAFS gives the chemical environmental information of the Fe center and Mössbauer spectroscopy confirms the 3 nm Nd-Fe-B-Na nanoparticle containing the Fe nanocluster. The possible magnetic coupling mechanism is proposed.

Colloidal magnetic nanoparticles (NPs) have attracted intensive research in the past decades from synthesis to various applications, ranging from ultrahigh density magnetic recording,^[1] single-electron tunneling magnetic device,^[2] magnetic energy storage,^[3] biomedical applications,^[4-6] and magnetic separable catalysis,^[7] to magnetically responsive photonic crystals.^[8] As a potential candidate to realize ultrahigh-density recording at single particle level, the essential prerequisite for practical one particle one bit of ultrahigh-density magnetic recording is to synthesize ultrasmall colloidal magnetic nanoparticles with enough high transition temperature. However, the blocking temperatures (T_B) of colloidal synthesized freestanding monodisperse magnetic nanoparticles and surfactant-assisted ball milled Nd₂Fe₁₄B nanoparticles with about 5 nm diameter based on long-range ferromagnetic interactions are far below room temperature, such as, 20-30K for 4-nm chemical disordered fcc FePt,^[1] 80K for 10-nm ϵ -Co,^[2b] 160 K for 5.2-nm CoFe₂O₄,^[4a] 25 K for 4-nm γ -Fe₂O₃,^[4b] 20 K for 1.8-nm CoPt₃,^[4c] 40 K for 5-nm Fe₃O₄,^[5a] and 65 K for 2.7-nm Nd₂Fe₁₄B.^[9a] At the same time, amorphous phase RE-TM and RE-TM-B alloys based on short-range ferromagnetic interactions (RE = rare-earth metal, TM = transition metals) with high magnetic anisotropy constant (K_u usually larger than 10^7 erg/cm³) have drawn much attentions for their commercial applications in magneto-optic sensor, high-density magneto-optic disk and high T_C .^[9b,9c,10-12] Short-range order structure and random magnetic anisotropy (RMA) of above mentioned amorphous ferromagnetic alloys inspire us that the undesirable effects of decreasing size on T_B do not behave as those of crystalline phase.

However, controlled synthesis of colloidal magnetic nanoparticles of amorphous phase metal alloys is a challenge. It is necessary to develop colloidal method to synthesize amorphous magnetic nanoparticles and investigate their magnetic properties at nanometer scale.

In this communication, we report controllable colloidal synthesis and magnetic properties of air-stable monodisperse amorphous Nd-Fe-B-Na nanoparticle, one of them with 3 nm in diameter and T_C higher than 650 K.

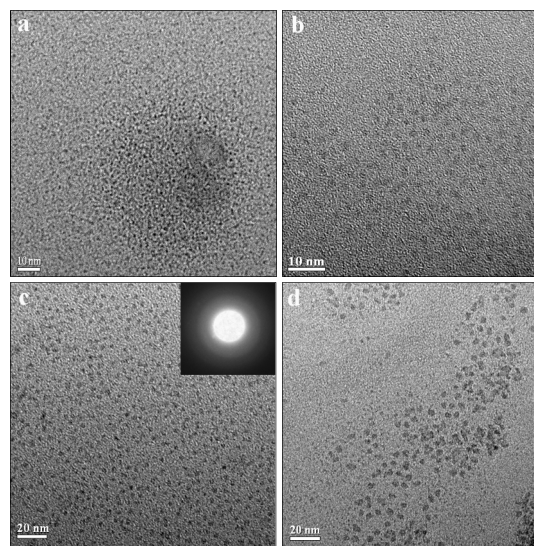


Figure 1 TEM characterizations of colloidal Nd-Fe-B-Na nanoparticles with different size. a, 1 nm; b, 2 nm; c, 3 nm; d, 5 nm.

To increase the ratio of magnetic centers, we try to eliminate sodium from the final product by selecting tetrabutylammonium borohydride (TBAB) and triethylamine borane complex. For the former, the reaction system produces a large amount of bubbles when the reducing agent is added in at 100 °C and no product is separable by centrifugation; for the later, triethylamine borane is sublimated on the cool part of glassware and no product can be

obtained. We also test KBH_4 and LiBH_4 : no reaction has been found for KBH_4 , but the reaction is very fast for LiBH_4 and no product is separable by centrifugation. The hydride, with low melting point (LiBH_4 , 275 °C) or compatible with organic phase (TBAB), react too fast to form stable nuclei before the dissociation of $\text{Nd}(\text{acac})_3$ and $\text{Fe}(\text{acac})_3$. Triethylamine borane complex are stable at the reflux temperature of the solvent and surfactants for its three B-C covalent chemical bonds. This could be the reason why superhydride (LiBEt_3H) has been selected to synthesize colloidal ϵ -Co nanoparticles: to form homogenous solution in organic phase (Dioctylether) and to avoid the possible incorporation of B atoms into ϵ -Co. In the series of LiBH_4 , NaBH_4 (m.p., 400 °C), and KBH_4 (m.p., 500 °C), only NaBH_4 can react steadily with the precursors and surfactants (OA and OM) in organic solution near 300 °C to form stable nuclei and its solid state ensures the following growth process. Thus, the suitable chemical reactivity of NaBH_4 and its solid state at the selected aging temperature realize the reasonable separation between nucleation and growth. When the temperature increases to 275 °C, there are small bubbles in the reaction, which are the bubbling effects taking place through absorbing local latent heat released from the exothermic reactions involved in the nucleation and growth of magnetic nanoparticles. The bubbling effects facilitate the formation of a huge number of nuclei.^[13] The reactions in the system is rather complex. At least, amidation reaction between OA and OM, the dissociation of $\text{Nd}(\text{acac})_3$ and $\text{Fe}(\text{acac})_3$ (facilitated by surfactants, such as OA and OM, and/or by hydride), and the reduction of $\text{Fe}(\text{III})$ by borohydride are involved.^[14] Because of the very high positive redox potential of metal Nd, NaBH_4 cannot reduce $\text{Nd}(\text{III})$ to Nd, supported by the XPS peak of Nd $3d_{5/2}$ at 982 eV, being the same value of Nd_2O_3 (see Supplementary Information, Figure S3). Even this reduction reaction occurs, the water molecules from the above-mentioned amidation reaction and OA can oxidize it to $\text{Nd}(\text{III})$. Considering the intrinsic oxophilic properties of $\text{Nd}(\text{III})$ and the presence of water and other oxygen-containing molecular species, the Nd-Fe-B-Na nanoparticles could contain some oxygen. These factors can contribute to the chemical stability to air, evaluated by the magnetic properties in the following part. These chemical reactions are different from the sputter deposition and melt spinning techniques on chemical composition control. We speculate that the reasons to form amorphous colloidal nanoparticles instead of crystalline ones are listed as follows. Firstly, the chemical potentials of the monomers (reactive atomic or molecular species) are usually high, and according to Ostwald's rule, the kinetically favoured metastable amorphous phase forms first.^[15] Secondly, the presence of $\text{Nd}(\text{III})$, sodium, some oxygen, and high content of boron could suppress the formation of crystalline phase. Thirdly, the temperature allowing us to synthesize ultrasmall and monodisperse nanoparticles (300-320 °C) is not high enough to rearrange and anneal the constituent atoms during growth. This rearrangement is usually associated with significant high thermal barriers.^[16] It is worth to note that it is likely a trend that ultrasmall nanoparticles adopt disordered structure compared to their bulk crystalline phases, such as chemically disordered face-centered cubic (fcc) for FePt colloidal nanocrystals,^[11] $(\gamma\text{-Fe}_2\text{O}_3)_{0.8}(\text{Fe}_3\text{O}_4)_{0.2}$ for Fe_3O_4 nanocrystals with diameter of 5 nm,¹⁰ and non-periodic and lack long-range atomic ordered structure of the Co and FeCo nanoparticles.^[17]

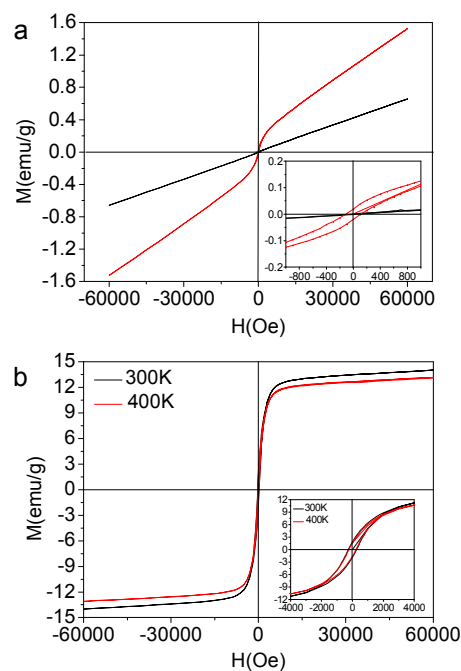


Figure 2 Magnetic properties of colloidal Nd-Fe-B-Na nanoparticles with different size. a, magnetic hysteresis of nanoparticle with 1 nm diameter (black curve) and 2 nm (red curve). b, magnetic hysteresis of nanoparticle with 3 nm diameter at 300 K (black curve) and 400 K (red curve).

The magnetic properties of the Nd-Fe-B-Na colloidal nanoparticles with size being 1 nm, 2 nm, and 3 nm corresponding to Figure 1 are measured with a SQUID-VSM system (MPMS, Quantum) in the temperature range lower than 400 K. The M-H magnetic hysteresis curves are depicted in Figure 2. The linear paramagnetic characterization is for the colloidal nanoparticle with 1 nm diameter. When the diameter increases to 2 nm, the ferromagnetic magnetic hysteresis loop is observed, with coercive field (H_c) being 120 Oe at 300 K (Figure 2a). The coercive field (H_c) of nanoparticles with 3 nm diameter is 262 Oe at 300K, 245 Oe at 400 K (Figure 2b). These H_c values are higher than that of bulk amorphous alloy measured at 300 K, about 10 Oe for $\text{Nd}_8\text{Fe}_{72}\text{B}_{20}$.^[12d] The saturation magnetization (M_s) at 6 T is 14 emu/g, comparable with that of Fe_3O_4 nanoparticles with the same size^[5c] which can exclude the possibility of the ferromagnetic properties originating from defect magnetism. In Figure 2, the time for the M-H measured at 400 K is twenty days later than the M-H curve measured at 300 K. From the M-H curve at 300 K in Figure 2b inset, we can see that the magnetic nanoparticles with 3 nm diameter cannot spontaneously magnetize or induced by the magnetic bar during colloidal synthesis. However, after the magnetic measurement at 300 K, the nanoparticle maintains its magnetic remanence at least for twenty days, as shown in Figure 2b inset for the M-H curve at 400 K. The stability in air of the Nd-Fe-B-Na colloidal nanoparticles is interrogated by the change of the magnetic properties after being exposed to air for two months. The coercive field (H_c) and magnetic remanence (M_r) decrease only by 0.5 percent, while the saturation magnetization (M_s) at 6 T decreases by 2.5 percent (see Supplementary Information, Figure S4). These indicate that the 3 nm nanoparticles are stable in air. **The magnetic property decreasing after exposing to air several day are due to the oxidation of the trace surface unstable Fe (e.g., $\text{Fe}(\text{I})$ and $\text{Fe}(\text{II})$) or $\text{Fe}(\text{O})$ nanocluster.**

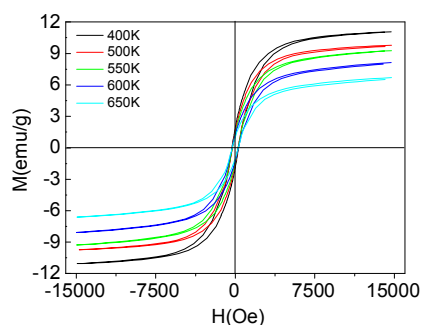


Figure 3 Magnetic properties of colloidal Nd-Fe-B-Na nanoparticles with 3 nm diameter at high temperature between 400 K and 650 K.

To shed more light on the structure and mag The magnetic properties of the 3 nm nanoparticle under temperature higher than 400 K are determined by LakeShore 7407 vibrating sample magnetometer (VSM) equipped with Hall probe. The M-H magnetic hysteresis curves and the magnetic parameters are given in Figure 3. As the temperature of the sample increases to 650 K, the saturation magnetization and magnetic remanence decrease. However, the coercive field (H_c) decreases some first and then increases a little, from 308 Oe to 270 Oe, and then to 293 Oe (see Supplementary Information, Figure S5). We do not measure the magnetic properties at the temperature higher than 650 K for the following considerations, higher temperature would decompose the organic surfactants (OA and OM) and result in the aggregation by annealing and sintering. The thermal analysis of the colloidal magnetic nanoparticles under nitrogen atmosphere is conducted (see Supplementary Information, Figure S6). There are an endothermic peak of DSC curve and a weight loss peak of TGA curve near 723 K, and these peaks can be tentatively assigned to the corresponding process of the decomposition of the organic surfactants of OA and OM and the fusion and aggregation of the nanoparticles. The magnetic properties at the temperature higher than 650 K would arise from the fusion and aggregation of the ‘naked’ nanoparticles, not at the single nanoparticle level. When the size increases to 5 nm (Figure 1d), the magnetic nanoparticles can spontaneously magnetize or induced by the magnetic bar during colloidal synthesis, shown in Figure S7. The coercive field (H_c) and magnetic remanence (M_r) are 612 Oe and 11.2 emu/g measured by LakeShore 7407 VSM at 300 K, while the saturation magnetization (M_s) at 1.8 T is 29.6 emu/g.

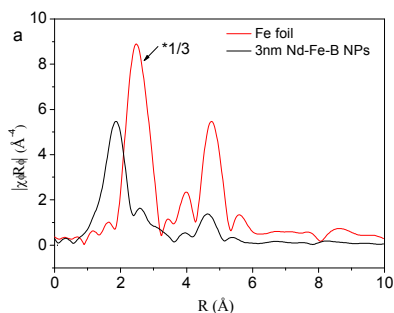


Figure 4 RDF's of the 3-nm Nd-Fe-B-Na nanoparticles and standard Fe foil.

Magnetic properties of the 3 nm Nd-Fe-B-Na nanoparticle, we perform Extended X-ray absorption fine structure (EXAFS) and Mössbauer spectroscopy characterization. The radial distribution functions (RDF) of the 3 nm Nd-Fe-B-Na nanoparticle and Fe foil,

obtained from their $k^3\chi(k)$ by Fourier transform in Figure S8, are depicted in Figure 4. There are several distinct peaks of the sample. Compare with the peaks of Fe foil, the peaks at 2.58 Å, 3.9 Å, and 4.6 Å of the sample can partially result from the Fe⁰ nanocluster. The peak at 1.86 Å can be assigned to the amorphous phase. Structure parameters obtained by fitting the Fe K-edge data shown in Figure 4 are listed in Table S1. There are about 3.5 boron atoms and 1.2 Fe atoms around each Fe center. The nearest Fe-B and Fe-Fe distances are 1.99 Å and 2.91 Å. There are EXAFS characterizations on Nd₂Fe₁₄B nanomagnets and nanocomposites, but they are of crystalline and short of the fitted results of Fe-B and Fe-Fe chemical bonds. It's difficult to directly compare the crystalline phase with amorphous phase. The distance of Fe-B is shorter, while the distance of Fe-Fe is larger than those of the amorphous Fe-Si-B alloy, 2.27 Å and 2.54 Å, respectively.^[11b] The first peak in the RDF of the 3 nm nanoparticle is in slightly higher position than those of standard Fe₂O₃ and Fe₃O₄ in Figure S9, indicating the Fe-B bonds being slightly larger than the Fe-O chemical bonds.

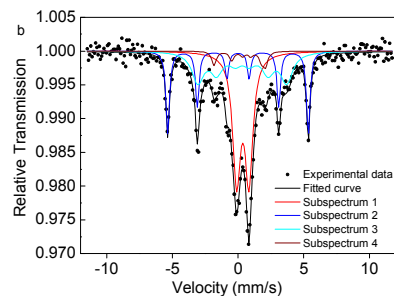


Figure 5 ⁵⁷Fe Mössbauer spectrum of the 3-nm Nd-Fe-B-Na nanoparticles measured at 300 K.

⁵⁷Fe Mössbauer spectroscopy of the sample measured at 300 K in Figure 5 and Table S2 confirms that there is a sextet subspectrum of subarea of 24 % (Subspectrum 2) with the same isomer shift (δ) as that of Fe foil and a hyperfine field of 33.3 kOe attributed to unoxidized Fe⁰ nanoparticles in a blocked state, assigned to Fe⁰ nanocluster(s).^[18] To exclude the possibility of the sextet subspectrum resulting from very large Fe nanoparticles not observed by TEM, we characterize the dynamic light scattering (DLS) of the 3 nm Nd-Fe-B-Na nanoparticles dispersed in hexane, there is no signal of particles with hydrodynamic diameter larger than 7 nm (Figure S10). For freestanding colloidal Fe nanoparticle, the blocking temperature of unoxidized 4.5 nm Fe nanoparticles is just 110 K.^[19] We speculate that the sextet subspectrum of the Fe⁰ nanocluster(s) could originate from their exchange-coupling with the amorphous parts surrounding them inside the 3 nm Nd-Fe-B-Na nanoparticle. This structure feature is in accordance with the RDF of the nanoparticles in Figure 4. Although the temperature to measure Mössbauer effect is far below T_C , there is still a doublet peak with 40 % subarea. This phenomenon is different from the magnetic behavior of CoFe₂O₄ nanocrystals and Fe nanocube assembly with only one sextet peak under the blocking temperature, probably due to structure disorder and surface effect.^[4a,18] Because of the surface effect and complex chemical composition, the Mössbauer spectra are also different from those of bulk amorphous Fe-B-Si, the bulk without any doublet peak.^[11b] However, there is no signal of Fe⁰ nanocluster in the 5 nm nanoparticles shown in Figure S11 and

Table S3, probably due to higher synthetic temperature being able to destroy the Fe nanocluster by forming Fe-B chemical bonds. As the size increases to 5 nm, the subarea of the doublet peak from Fe nuclei with unblocked state decreases slightly to 37 %. For the nanoparticles with 1 nm or 2 nm, there are only two doublet peaks, although the H_c is 120 Oe of the 2 nm one (Figure S11 and Table S3).

For the present colloidal Nd-Fe-B-Na nanoparticles, when the size decreases to 1 nm, the zero-field-cooling (ZFC) magnetization (Figure S12) under 1000 Oe magnetic field indicates that there is no peak magnetization between 2 K and 305 K, unlike those of ϵ -Co, CoFe_2O_4 , and Fe_3O_4 magnetic nanoparticles.^[1,4a,5a] These results probably arise from finite size effects suppressing the magnetic ordering. Considering the ferromagnetic properties of the magnetic nanoparticles larger than 2 nm (Figure 2a, red curve), the size is the crucial factor to determine the magnetic exchange model. The critical size of the present colloidal Nd-Fe-B-Na nanoparticle from the experimental results should be between 1 nm and 2 nm, which is close to the estimated grain size of Gd-Co amorphous films (smaller than 25 Å) and the diameter of Fe-enriched clusters simulated in the inhomogeneous $\text{Fe}_{67}\text{Y}_{33}$ alloys (about 15–20 Å).^[10a,11a]

Conclusions

In summary, the controlled colloidal synthesis of amorphous Nd-Fe-B-Na nanoparticles and the size dependence of the magnetic properties have been demonstrated in sub-5-nm regime. The magnetic nanoparticle with 3 nm diameter exhibit ferromagnetic magnetic properties even at temperature as high as 650 K. The structure of the 3 nm Nd-Fe-B-Na nanoparticles has been characterized by EXAFS and Mössbauer spectroscopy. These characteristics clearly demonstrate that such Nd-Fe-B-Na nanoparticles present opportunities for fundamental studies of nanomagnetism, as well as for potential ultrahigh density magnetic recording, permanent magnetic nanocomposites, catalysis, and biological applications. The present colloidal method can also be used to grow colloidal nanoparticles of other amorphous metal alloys with nanometer size, with potential importance in magnetic, magneto-optic, and electronic applications.

Acknowledgements

This work is supported by the National Natural Science Foundation of China (91122003) and Developing Science Funds of Tongji University.

Notes and references

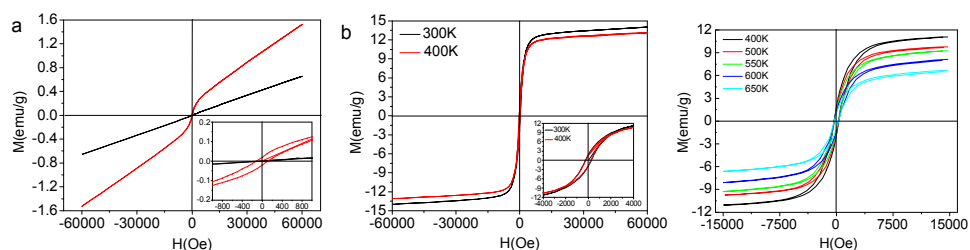
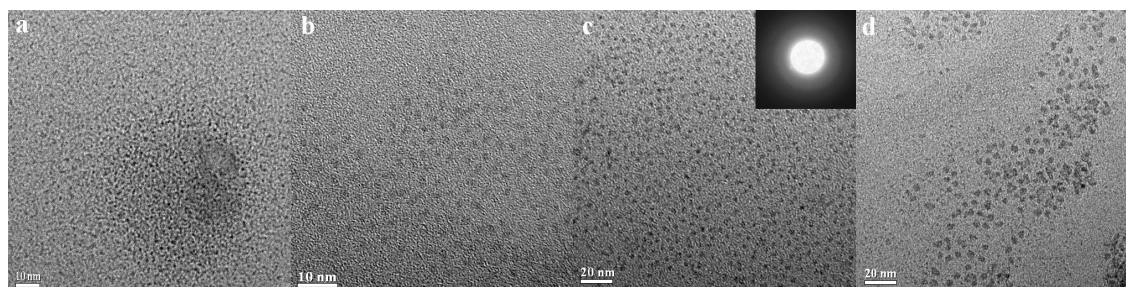
^a Department of Chemistry, Tongji University, Shanghai 200092, P. R. China. Fax: (+86) 21-65982287; E-mail: byan@tongji.edu.cn; b

^b Shanghai Synchrotron Radiation Facility, Shanghai Institute of Applied Physics, Chinese Academy of Sciences, Shanghai 201204, China

† Electronic Supplementary Information (ESI) available: [details of any supplementary information available should be included here]. See DOI: 10.1039/c000000x/

- 1 S. H. Sun, C. B. Murray, D. Weller, L. Folks and A. Moser, *Science*, 2000, **287**, 1989.
- 2 (a) S. H. Sun and C. B. Murray, *J. Appl. Phys.*, 1999, **85**, 4325; (b) C. T. Black, C. B. Murray, R. L. Sandstrom and S. H. Sun, *Science*, 2000, **290**, 1131; (c) V. F. Puentes, K. M. Krishnan and A. P. Alivisatos, *Science*, 2001, **291**, 2115.
- 3 H. Zeng, J. Li, J. P. Liu, Z. L. Wang and S. H. Sun, *Nature*, 2002, **420**, 395.
- 4 (a) C. Liu, B. S. Zou, A. J. Rondinone and J. Zhang, *J. Am. Chem. Soc.*, 2000, **122**, 6263; (b) T. Hyeon, S. S. Lee, J. Park, Y. Chung and H. Bin Na, *J. Am.*

- Chem. Soc.*, 2001, **123**, 12798; (c) J. I. Park and J. Cheon, *J. Am. Chem. Soc.*, 2001, **123**, 5743; (d) S. H. Sun and H. Zeng, *J. Am. Chem. Soc.*, 2002, **124**, 8204.
- 5 (a) J. Park, K. J. An, Y. S. Hwang, J. G. Park, H. J. Noh, J. Y. Kim, J. H. Park, N. M. Hwang and T. Hyeon, *Nat. Mater.*, 2004, **3**, 891; (b) J. Park, E. Lee, N. M. Hwang, M. S. Kang, S. C. Kim, Y. Hwang, J. G. Park, H. J. Noh, J. Y. Kim, J. H. Park and T. Hyeon, *Angew. Chem., Int. Ed.*, 2005, **44**, 2872; (c) B. H. Kim, N. Lee, K. An, Y. I. Park, Y. Choi, K. Shin, Y. Lee, S. G. Kwon, H. B. Na, J. G. Park, T. Y. Ahn, Y. W. Kim, W. K. Moon, S. H. Choi and T. Hyeon, *J. Am. Chem. Soc.*, 2011, **133**, 12624; (d) J. Dobson, *Nat. Nanotechnol.*, 2008, **3**, 139.
- 6 (a) C. Tassa, S. Y. Shaw and R. Weissleder, *Acc. Chem. Res.*, 2011, **44**, 842; (b) D. Yoo, J. H. Lee, T. H. Shin and J. Cheon, *Acc. Chem. Res.*, 2011, **44**, 863; (c) D. Ho, X. L. Sun and S. H. Sun, *Acc. Chem. Res.*, 2011, **44**, 875; (d) J. H. Lee, J. T. Jang, J. S. Choi, S. H. Moon, S. H. Noh, J. W. Kim, J. G. Kim, I. S. Kim, K. I. Park and J. Cheon, *Nat. Nanotechnol.*, 2011, **6**, 418.
- 7 (a) A. H. Lu, W. Schmidt, N. Matoussevitch, H. Bonnemann, B. Splithoff, B. Tesche, E. Bill, W. Kiefer and F. Schuth, *Angew. Chem.*, 2004, **43**, 4303; (b) M. Shokouhimehr, Y. Z. Piao, J. Kim, Y. J. Jang and T. Hyeon, *Angew. Chem., Int. Ed.*, 2007, **46**, 7039; (c) V. Mazumder, M. F. Chi, K. L. More and S. H. Sun, *J. Am. Chem. Soc.*, 2010, **132**, 7848; (d) Y. M. Lee, M. A. Garcia, N. A. F. Huls and S. H. Sun, *Angew. Chem. Int. Ed.*, 2010, **49**, 1271; (e) S. J. Guo, S. Zhang, X. L. Sun and S. H. Sun, *J. Am. Chem. Soc.*, 2011, **133**, 15354.
- 8 (a) J. P. Ge, Y. X. Hu and Y. D. Yin, *Angew. Chem., Int. Ed.*, 2007, **46**, 7428; (b) J. P. Ge, L. He, J. Goebel and Y. D. Yin, *J. Am. Chem. Soc.*, 2009, **131**, 3484; (c) J. P. Ge and Y. D. Yin, *Angew. Chem. Int. Ed.*, 2011, **50**, 1492; (d) Y. X. Hu, L. He and Y. D. Yin, *Angew. Chem., Int. Ed.*, 2011, **50**, 3747.
- 9 (a) N. G. Akdogan, W. F. Li and G. C. Hadjipanayis, *J. Appl. Phys.*, 2011, **109**, 07A759; (b) C. W. Kim, Y. H. Kim, U. Pal and Y. S. Kang, *J. Mater. Chem. C*, 2013, **1**, 275; (c) A. Hussain, A. P. Jadhav, Y. K. Baek, H. J. Choi, J. Lee and Y. S. Kang, *J. Nanosci. Nanotechnol.*, 2013, **13**, 7717.
- 10 (a) P. Chaudhari, J. J. Cuomo and R. J. Gambino, *Appl. Phys. Lett.*, 1973, **22**, 337; (b) Y. Togami, *Appl. Phys. Lett.*, 1978, **32**, 673; (c) R. Harris, M. Plischke and M. J. Zuckermann, *Phys. Rev. Lett.*, 1973, **31**, 160.
- 11 (a) D. Spisak, J. Hafner and R. Lorenz, *J. Magn. Magn. Mater.*, 1997, **166**, 303; (b) Y. Takahara and N. Narita, *Mat. Sci. Eng. A*, 2001, **315**, 153; (c) N. Hassanain, H. Lassri, R. Krishnan and A. Berrada, *J. Magn. Magn. Mater.*, 1995, **146**, 37; (d) N. Hassanain, H. Lassri, R. Krishnan and A. Berrada, *J. Magn. Magn. Mater.*, 1995, **146**, 315.
- 12 (a) M. Slimani, M. Hamedoun, H. Lassri, S. Sayouri and R. Krishnan, *J. Magn. Magn. Mater.*, 1996, **153**, 132; (b) M. Slimani, M. Hamdoun, M. Tlemcani, H. Arhouchi and S. Sayouri, *Physica B*, 1997, **240**, 372; (c) E. H. Sayouty, F. Annouar, H. Lassri, N. Randrianantoandro and J. M. Grenèche, *J. Alloys Compds.*, 2005, **397**, 47; (d) N. Hassanain, H. Lassri, A. Berrada and R. Krishnan, *Phys. Stat. Sol. C*, 2006, **3**, 3239.
- 13 J. Lynch, J. Q. Zhuang, T. Wang, D. LaMontagne, H. M. Wu and Y. C. Cao, *J. Am. Chem. Soc.*, 2011, **133**, 12664.
- 14 (a) N. R. Jana, Y. F. Chen and X. G. Peng, *Chem. Mater.*, 2004, **16**, 3931; (b) J. Joo, S. G. Kwon, J. H. Yu and T. Hyeon, *Adv. Mater.*, 2005, **17**, 1873; (c) H. M. Wu, Y. G. Yang and Y. C. Cao, *J. Am. Chem. Soc.*, 2006, **128**, 16522; (d) H. T. Zhang, D. H. Ha, R. Hovden, L. F. Kourkoutis and R. D. Robinson, *Nano Lett.*, 2011, **11**, 188; (e) Q. Zhang, B. Yan, F. Lei and H. H. Chen, *Nanoscale* 2012, **4**, 7646.
- 15 W. Z. Ostwald, *Phys. Chem.*, 1897, **22**, 289.
- 16 L. E. M. Howard, H. L. Nguyen, S. R. Giblin, B. K. Tanner, I. Terry, A. K. Hughes and J. S. O. Evans, *J. Am. Chem. Soc.*, 2005, **127**, 10140.
- 17 (a) D. P. Dinega and M. G. Bawendi, *Angew. Chem., Int. Ed.*, 1999, **38**, 1788; (b) B. Chaudret, C. Desvieux, C. Amiens, P. Fejes, P. Renaud, M. Respaud, P. Lecante and E. Snoeck, *Nat. Mater.*, 2005, **4**, 750.
- 18 F. Dumestre, B. Chaudret, C. Amiens, P. Renaud and P. Fejes, *Science*, 2004, **303**, 821.
- 19 T. C. Monson, E. L. Venturini, V. Petkov, Y. Ren, J. M. Lavin and D. L. Huber, *J. Magn. Magn. Mater.*, 2013, **331**, 156.



Ultrasmall and monodisperse air-stable colloidal Nd-Fe-B nanoparticles have been synthesized by solution phase colloidal method and characterized by TEM and SQUID. The size of them can be controlled in sub-5-nm regime. The critical temperature (T_C) of Nd-Fe-B nanoparticle with 3 nm in diameter is surprisingly high, higher than 650 K. The possible magnetic coupling mechanism is proposed. EXAFS gives the chemical environmental information of the Fe center and Mössbauer spectroscopy confirms the 3 nm Nd-Fe-B nanoparticle containing the Fe nanocluster. The possible magnetic coupling mechanism is proposed.

SUPPLEMENTARY INFORMATION

Ultrasmall and monodisperse colloidal amorphous Nd-Fe-B-Na nanoparticles

with high T_C

Qiang Zhang, Zheng Jiang and Bing Yan*

Experimental section

Materials: Nd(acac)₃·xH₂O (99.99 %), Fe(acac)₃ (99 %), NaBH₄ (99 %) are adopted. Oleylamine (OM, C18:80~90%, Alfa Aesar), oleic acid (OA, 90 %, Alfa Aesar), and 1-Octadecene (ODE, > 90 %, Alfa Aesar) are used as starting materials without further purification. Tetrabutylammonium borohydride and triethylamine borane are selected as reducing agents.

Synthesis of colloidal Nd-Fe-B-Na nanoparticles with different size: In a typical synthesis for 3 nm nanoparticles, 0.25 mmol Nd(acac)₃ and 1.5 mmol Fe(acac)₃ are added to mixed solvent composed of 4 mL of oleylamine (OM), 2 mL oleic acid (OA), and 10 mL 1-Octadecene (ODE) at room temperature. The mixture is heated to 100 °C in a vacuum for 30 min to remove water and oxygen. Then, the powder of 2.5 mmol NaBH₄ is swiftly added in under Ar atmosphere. The mixture is heated to 310 °C over approximately 4.5 min under Ar atmosphere, aging for 6 min. After air cooling the three-necked flask by taking off the temperature-controlled electromantle, the nanosheets are precipitated with ethanol, redispersed in cyclohexane for the transmission electron microscopy (TEM) characterizations and dried in a vacuum overnight for other measurements. One batch allows us to obtain about 0.3 g colloidal nanoparticles. For the nanoparticles with 1 nm or 2 nm, the temperature and aging time are selected as 300 °C and without aging or aging for 6 min, respectively.

For the synthesis for 5 nm nanoparticles, the mixed solvent composed of 2 mL of oleylamine (OM), 1 mL oleic acid (OA), and 5 mL 1-Octadecene (ODE) is selected, while other parameters are kept identical. The mixture is heated to 320 °C, aging for 10 min.

Characterization: XRD patterns are recorded with a Bruker D8 diffractometer using Cu K α radiation with 40 mA and 40 kV. Transmission electron microscope (TEM), energy-dispersive X-ray spectroscopy (EDS), and selected area electron diffraction (SAED) are carried out on a JEOL JEM-2010F electron microscope operated at 200 kV. XPS experiments were carried out on a Perkin Elmer PHI-5000C ESCA system with Mg K α radiation ($h\nu=1253.6$ eV) under a base pressure of 10⁻⁹ Torr.

The analysis of Nd, Fe, B, and Na is performed on the Perkin Optima 2100DV Inductively Coupled Plasma Optical Emission Spectrometer (ICP-OES). The magnetic properties at temperature lower than 400 K are measured with a SQUID-VSM system (MPMS, Quantum), which adopts the new FastLab data acquisition technique and the QuickSwich magnetic control technique. The magnetic properties at temperature higher than 400 K are measured with a LakeShore 7407 vibrating sample magnetometer (VSM) with Hall probe. X-ray absorption fine structure (XAFS) spectra are measured at the BL14W1 beamline of the Shanghai Synchrotron Radiation Facility (SSRF) with a ring current of 200-300 mA at 3.5 GeV. Data are recorded in transmission mode using a Si(111) double crystal monochromator. Fe K-edge XAFS data are analyzed using standard procedures with the program IFEFFIT. ⁵⁷Fe Mössbauer spectra are measured under constant acceleration transmission mode with a ⁵⁷Co/Rh source. The velocity is calibrated by a 25 μ m thick α -Fe foil, and the Isomer Shift (I.S.) is relative to the center of α -Fe foil at 300 K. The spectra are analyzed using MossWinn.^[2] Thermogravimetric analysis (TGA) and differential scanning calorimetry (DSC) are simultaneously performed on a Netzsch STA 409 at a heating rate of 5 K/min under nitrogen atmosphere. Dynamic light scattering (DLS) measurement is analyzed on a Nanotrac 250 analyzer by dispersing the 3 nm Nd-Fe-B-Na nanoparticles in hexane.

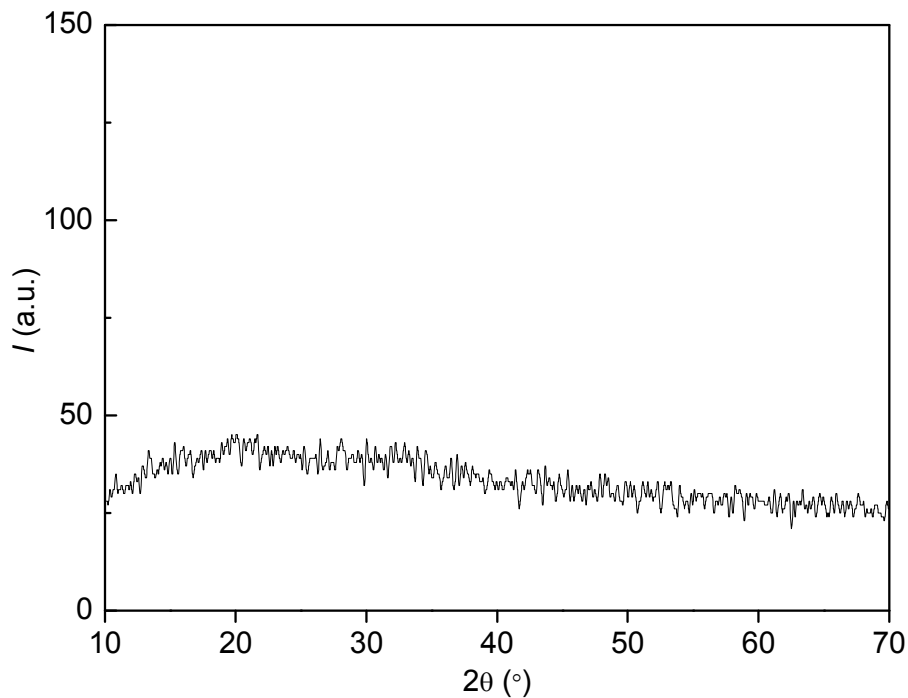


Figure S1 XRD pattern of the 3-nm Nd-Fe-B-Na nanoparticles.

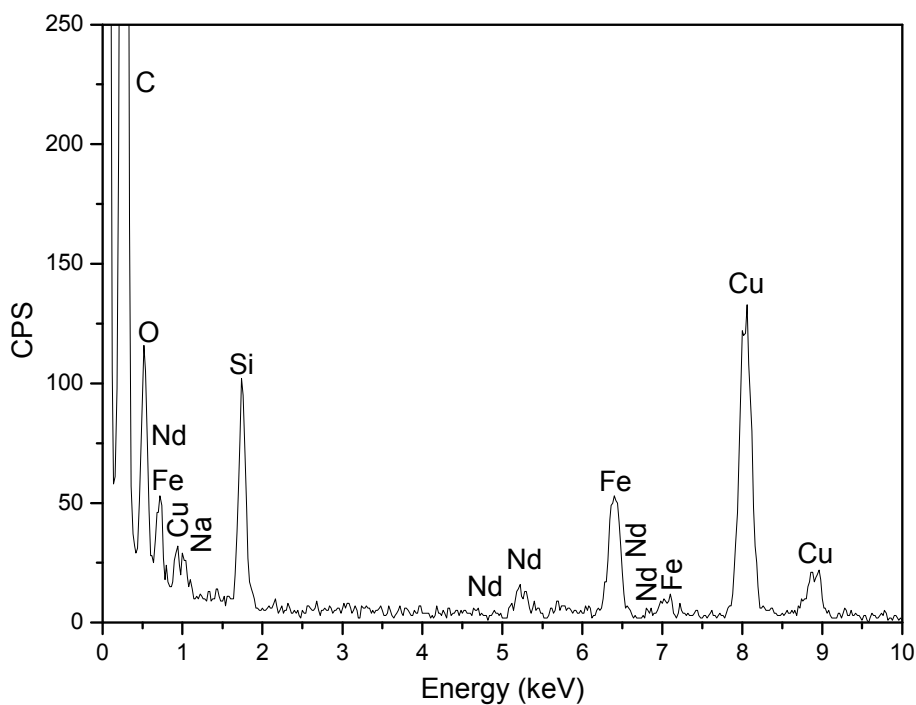


Figure S2 EDS of colloidal Nd-Fe-B-Na nanoparticles with 3 nm diameter, corresponding to the TEM image in Figure 1c in the main text. Cu and carbon elements are coming from the holey carbon film coated Cu grid supporting sample during EDS measurement. The signal of B is overlapped with that of carbon element. Si and O signals are probably from SiO₂ contaminant, for

no signals of Si element in XPS spectrum in Figure S3.

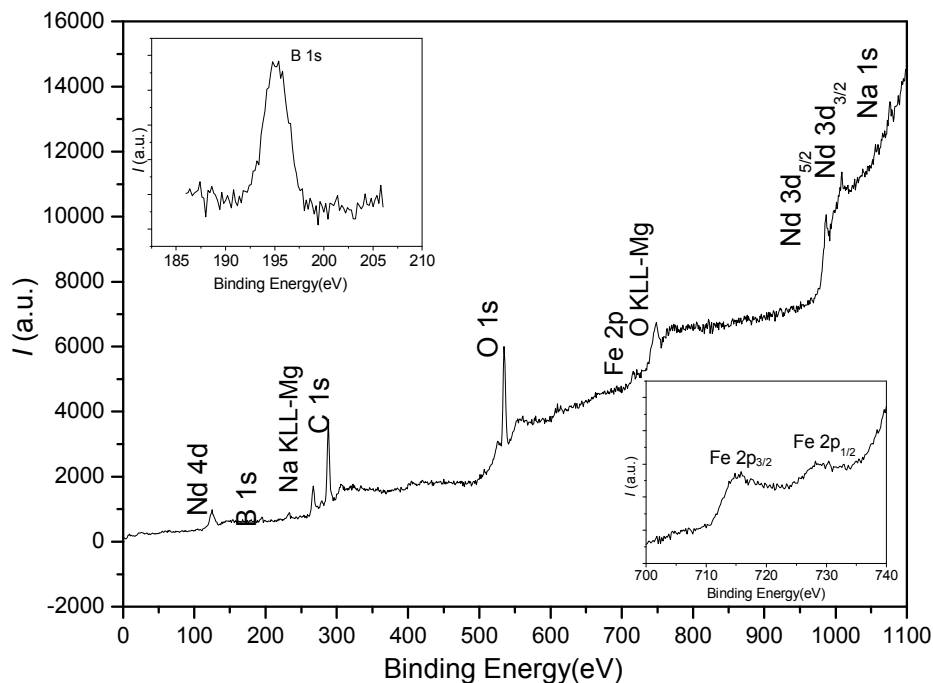


Figure S3 XPS spectrum of colloidal Nd-Fe-B-Na nanoparticles with 3 nm diameter.

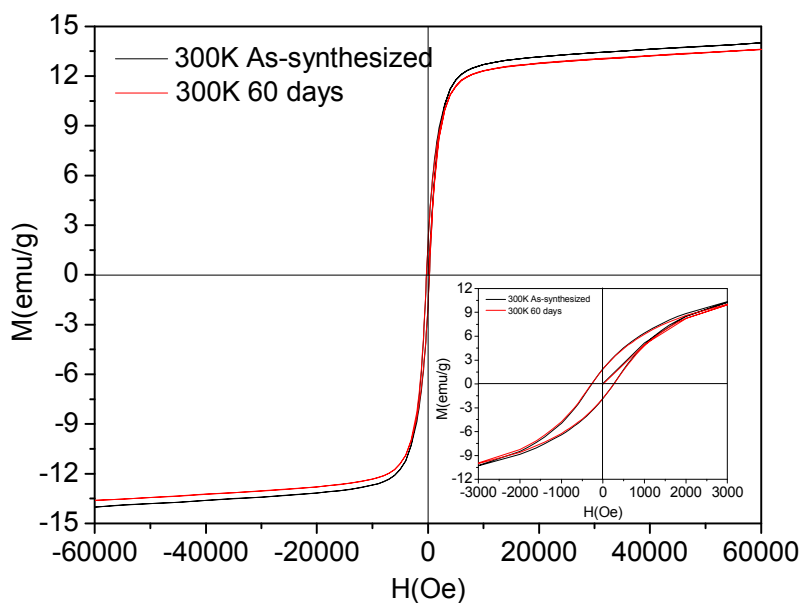


Figure S4 Magnetic properties of colloidal Nd-Fe-B-Na nanoparticles with 3 nm diameter.

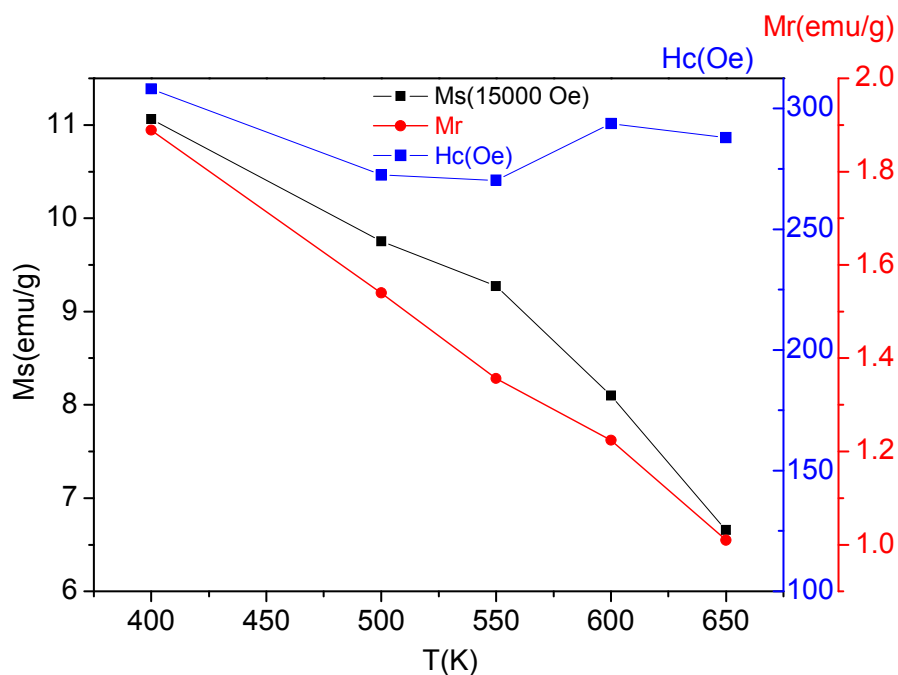


Figure S5 Graphic presentation of the magnetic parameters in Figure 3 in the main text.

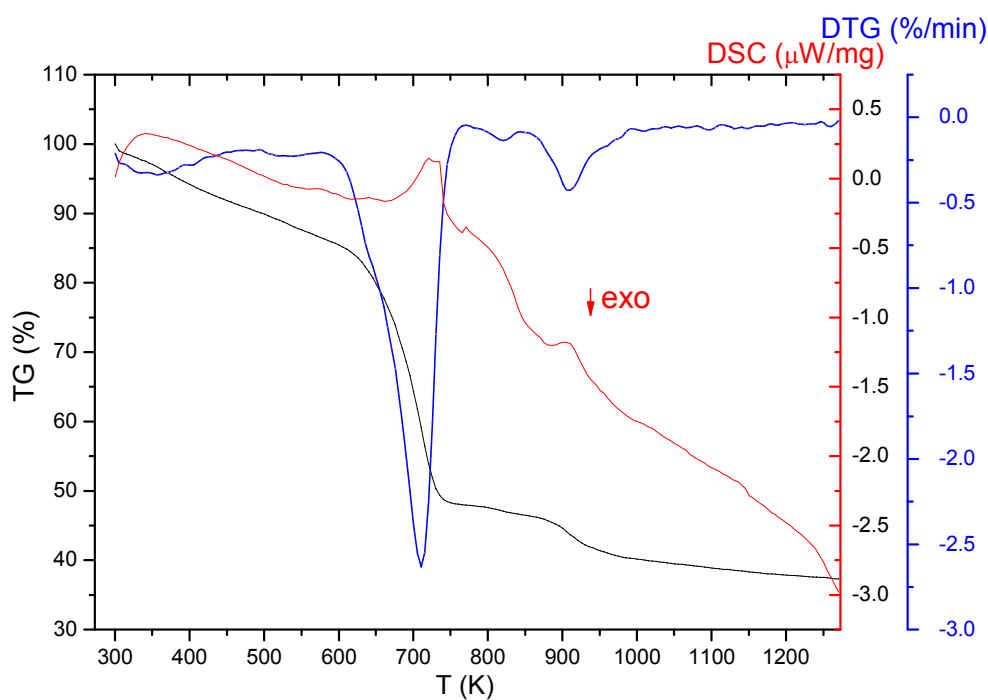


Figure S6 The thermogravimetric analysis (TG) (black curve), differential scanning calorimetry (DSC) (red curve) and differential thermogravimetric analysis (DTG) (blue curve) for colloidal Nd-Fe-B-Na nanoparticles with 3 nm diameter under N₂ atmosphere.

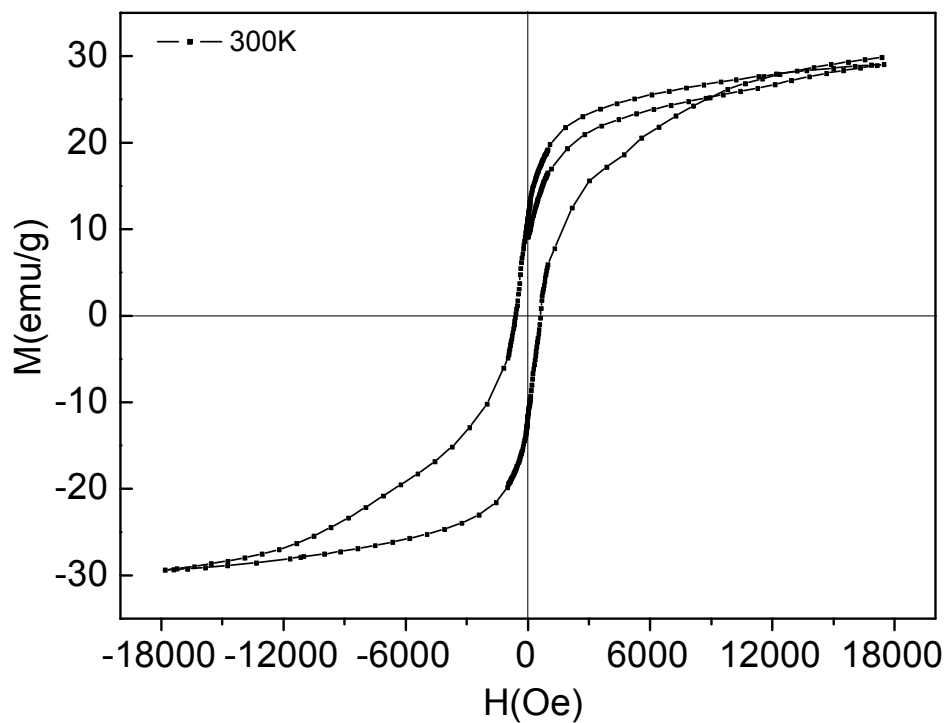


Figure S7 Magnetic properties of colloidal Nd-Fe-B-Na nanoparticles with 5 nm diameter at 300 K measure by LakeShore 7407 vibrating sample magnetometer (VSM).

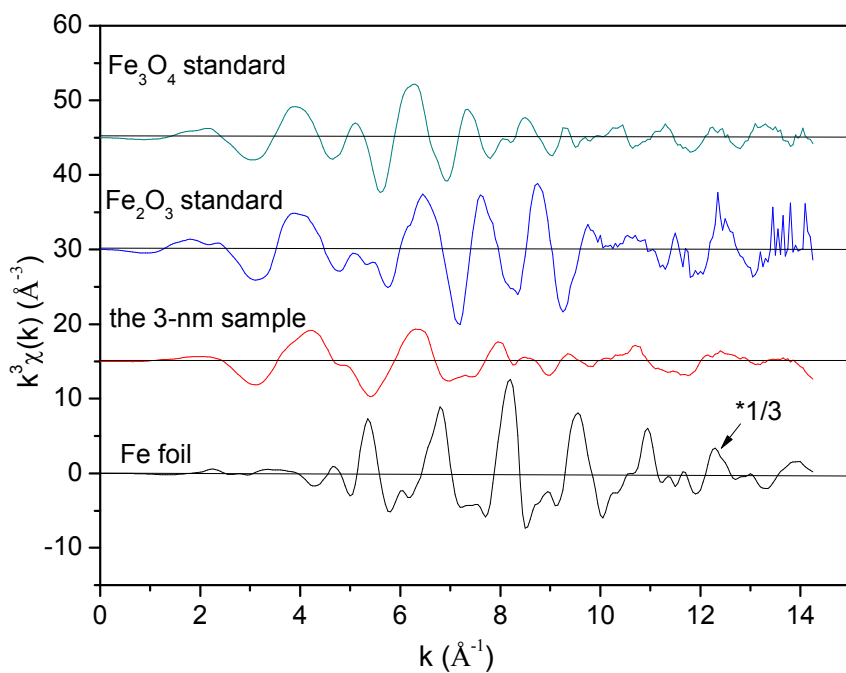
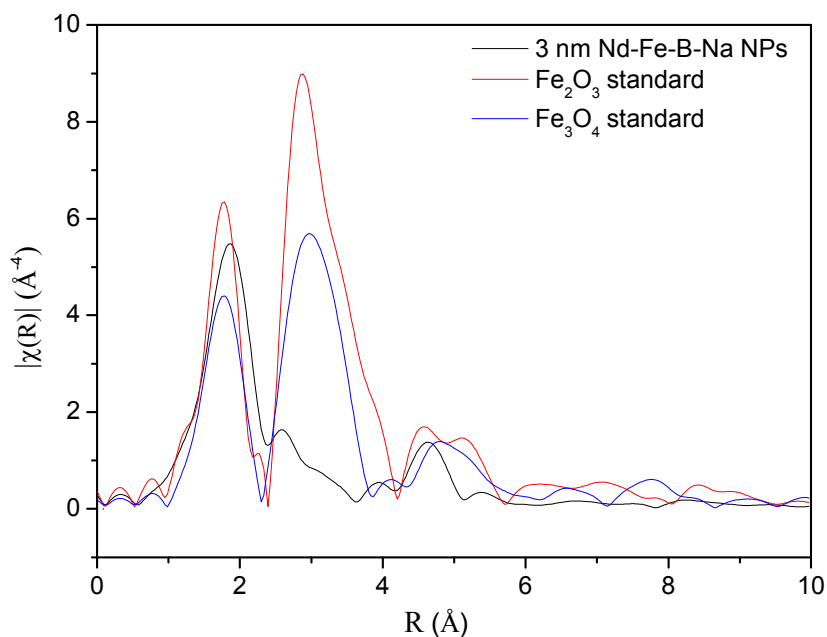


Figure S8 Fe K -edge k^3 -weighted experimental EXAFS spectra of the Fe foil, the 3-nm sample, Fe₂O₃ standard, and Fe₃O₄ standard.

Table S1 Structural parameters obtained by fitting the Fe *K*-edge EXAFS data shown in Figure 4 in the main text.^a

Sample	Terms	N	R (Å)	σ^2 (Å ²)	R_f
3nm	Fe-B ^b	3.5	1.99	0.004	0.026
Nd-Fe-B-Na NPs	Fe-Fe	1.2	2.91	0.008	

^a N is the coordination number, R is the coordination distance, σ^2 is the Debye Waller (disorder) term, and R_f is a measure of the goodness of fit. ^b There are the Fe-O and Fe-N chemical bonds on the surface of the nanoparticles by Fe coordinating with oleate, oleic acid, and oleylamine.

**Figure S9** RDF's of the 3-nm Nd-Fe-B-Na nanoparticles, standard Fe₂O₃, and Fe₃O₄ transformed from the data from Figure S8.**Table S2.** ⁵⁷Fe Mössbauer hyperfine parameters for the 3-nm Nd-Fe-B-Na nanoparticles at 300 K.^a

Sample (Nd-Fe-B-Na NPs)	Temp (K)	Subspectra	Isomer shift δ^b (mm/s)	quadrupolar splitting, ΔE_q (mm/s)	hyperfine field median value, (B_{hf}) (T)	Area _{spectrum} (%)
3nm	300	1	0.36 (1)	0.94(1)	-	40.2
		2	0.00(1)	-	33.3(1)	24.6
		3	0.32(4)	-	21.0(3)	30.0
		4	0.39(7)	-0.52(1)	12.2(3)	5.2

^a Errors on the last digits are given within parentheses. ^b Referred to metallic iron, α -Fe.

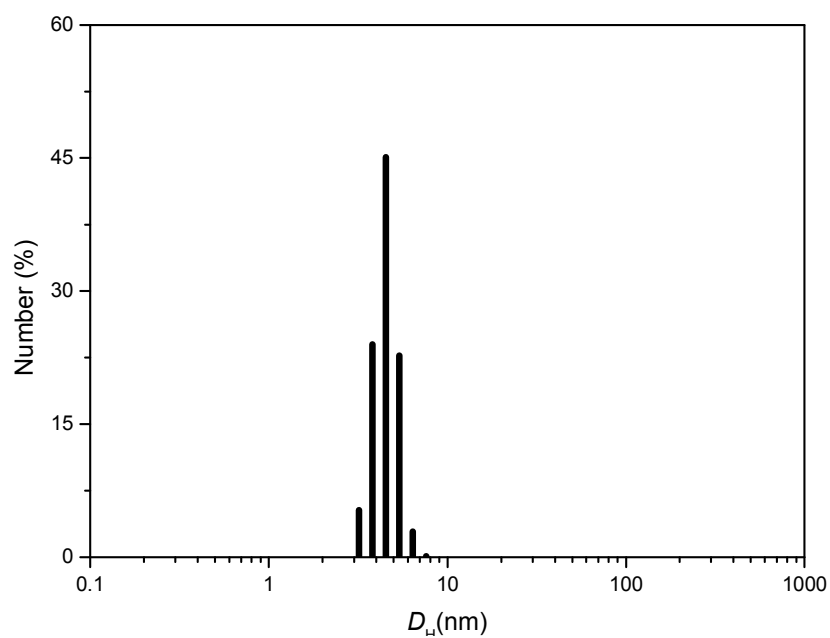
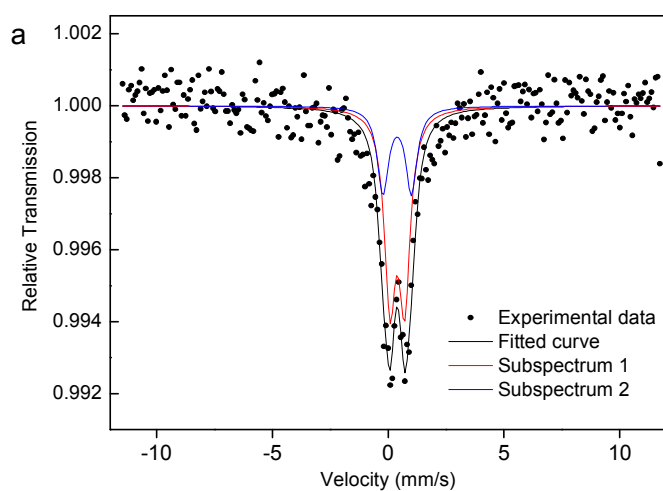


Figure S10 Hydrodynamic diameters measured by dynamic light scattering (DLS) for the 3-nm Nd-Fe-B-Na nanoparticles dispersed in hexane.



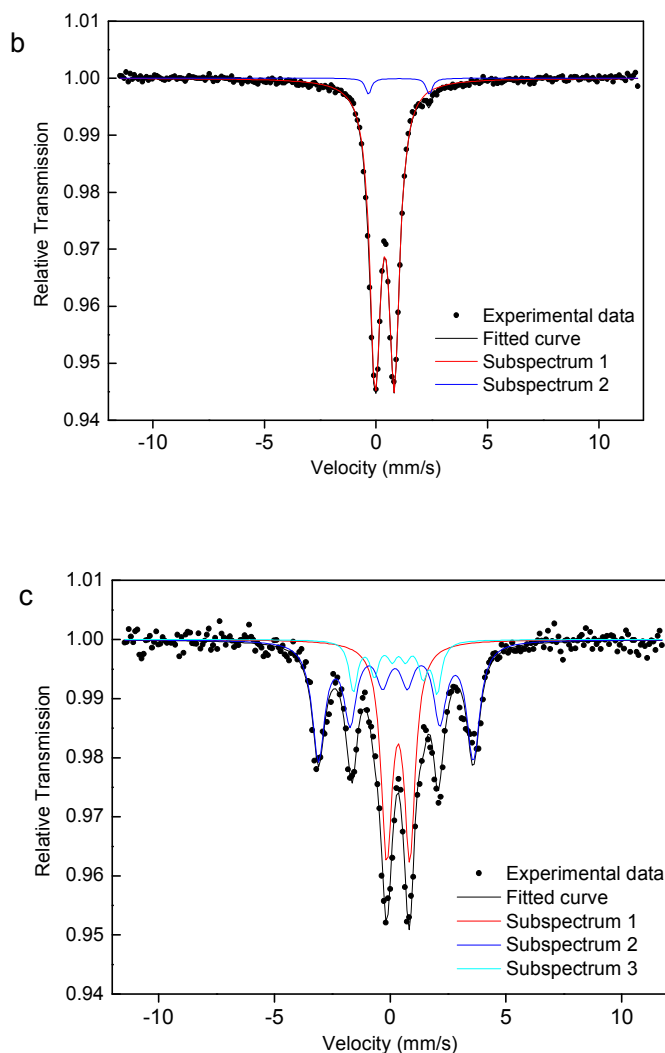


Figure S11 ^{57}Fe Mössbauer spectrum of the Nd-Fe-B-Na nanoparticles with different size measured at 300 K. a, 1 nm; b, 2 nm; c, 5 nm.

Table S3. ^{57}Fe Mössbauer hyperfine parameters for the Nd-Fe-B-Na nanoparticles with different diameter at 300 K. ^a

Sample (Nd-Fe-B -Na NPs)	Temp (K)	Subspectra	Isomer shift δ^b (mm/s)	quadrupolar splitting, ΔE_q (mm/s)	hyperfine field median value, (B_{hf}) (T)	Area _{subspectrum} (%)
1 nm	300	1	0.40(1)	0.63(2)	-	68.4
		2	0.39(3)	1.2(1)	-	31.6
2 nm	300	1	0.397(1)	0.863(1)	-	97.0
		2	1.03(1)	2.73(2)	-	3.0
5 nm	300	1	0.35(1)	1.00(1)	-	37.4
		2	0.23(1)	0.04(1)	20.8(1)	48.6
		3	0.30(2)	-0.15(3)	11.3(1)	14.0

^a Errors on the last digits are given within parentheses. ^b Referred to metallic iron, α -Fe.

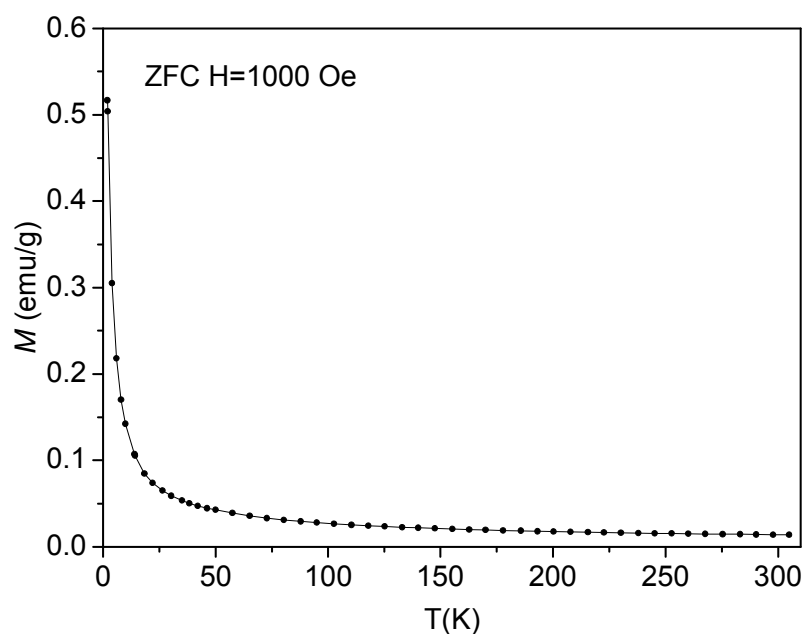


Figure S12 The zero-field-cooling (ZFC) magnetization curve of 1 nm colloidal Nd-Fe-B-Na nanoparticles under 1000 Oe magnetic field at the temperature between 2 K and 305 K.

Reference

- [1] M. Newville, IFEFFIT: interactive XAFS analysis and FEFF fitting. *J. Synchrotron Radiat.*, **2001**, *8*, 322-324.
- [2] Z. Klencsár, E. Kuzmann, A. Vértes, User-friendly software for Mössbauer spectrum analysis, *J. Radioanal. Nucl. Chem.*, **1996**, *210*, 105-118.

COMMUNICATION

Ultrasmall and monodisperse colloidal amorphous Nd-Fe-B-Na magnetic nanoparticles with high T_C

Cite this: DOI: 10.1039/x0xx00000x

Q. Zhang^a, Z. Jiang^b and B. Yan^a

Received 00th January 2012,

Accepted 00th January 2012

DOI: 10.1039/x0xx00000x

www.rsc.org/

Abstract Ultrasmall and monodisperse air-stable colloidal Nd-Fe-B-Na nanoparticles (NPs) have been synthesized by solution phase colloidal method and characterized by TEM, EXAFS, Mössbauer spectroscopy, and SQUID. The size of them can be controlled in the sub-5-nm regime. The critical temperature (T_C) of Nd-Fe-B-Na nanoparticle with 3 nm in diameter is surprisingly high, higher than 650 K. EXAFS gives the chemical environmental information of the Fe center and Mössbauer spectroscopy confirms the 3 nm Nd-Fe-B-Na nanoparticle containing the Fe nanocluster. The possible magnetic coupling mechanism is proposed.

Colloidal magnetic nanoparticles (NPs) have attracted intensive research in the past decades from synthesis to various applications, ranging from ultrahigh density magnetic recording,^[1] single-electron tunneling magnetic device,^[2] magnetic energy storage,^[3] biomedical applications,^[4-6] and magnetic separable catalysis,^[7] to magnetically responsive photonic crystals.^[8] As a potential candidate to realize ultrahigh-density recording at single particle level, the essential prerequisite for practical one particle one bit of ultrahigh-density magnetic recording is to synthesize ultrasmall colloidal magnetic nanoparticles with enough high transition temperature. However, the blocking temperatures (T_B) of colloidally synthesized freestanding monodisperse magnetic nanoparticles and surfactant-assisted ball milled Nd₂Fe₁₄B nanoparticles with about 5 nm diameter based on long-range ferromagnetic interactions are far below room temperature, such as, 20-30K for 4-nm chemical disordered fcc FePt,^[1] 80K for 10-nm ϵ -Co,^[2b] 160 K for 5.2-nm CoFe₂O₄,^[4a] 25 K for 4-nm γ -Fe₂O₃,^[4b] 20 K for 1.8-nm CoPt₃,^[4c] 40 K for 5-nm Fe₃O₄,^[5a] and 65 K for 2.7-nm Nd₂Fe₁₄B.^[9a] At the same time, amorphous phase RE-TM and RE-TM-B alloys based on short-range ferromagnetic interactions (RE = rare-earth metal, TM = transition metals) with high magnetic anisotropy constant (K_u usually larger than 10^7 erg/cm³) have drawn much attentions for their commercial applications in magneto optic sensor, high-density magneto optic disk and high T_C .^[9b,9c,10-12] Short-range order structure and random magnetic anisotropy (RMA) of above mentioned amorphous ferromagnetic alloys inspire us that the undesirable effects of decreasing size on T_B do not behave as those of crystalline phase.

However, controlled synthesis of colloidal magnetic nanoparticles of amorphous phase metal alloys is a challenge. It is necessary to develop colloidal method to synthesize amorphous magnetic nanoparticles and investigate their magnetic properties at nanometer scale.

In this communication, we report controllable colloidal synthesis and magnetic properties of air-stable monodisperse amorphous Nd-Fe-B-Na nanoparticle, one of them with 3 nm in diameter and T_C higher than 650 K.

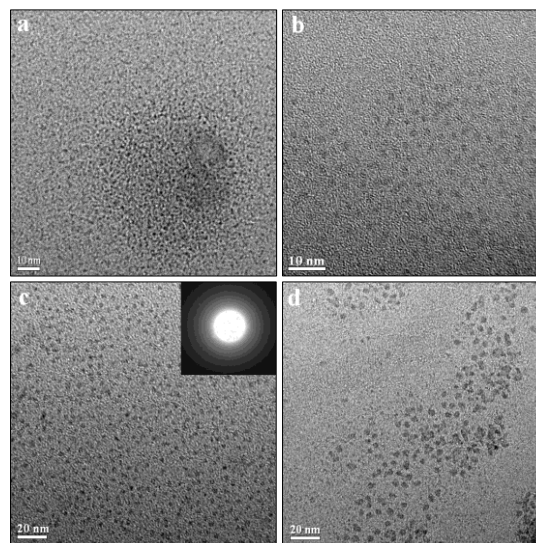


Figure 1 TEM characterizations of colloidal Nd-Fe-B-Na nanoparticles with different size. a, 1 nm; b, 2 nm; c, 3 nm; d, 5 nm.

To increase the ratio of magnetic centers, we try to eliminate sodium from the final product by selecting tetrabutylammonium borohydride (TBAB) and triethylamine borane complex. For the former, the reaction system produces a large amount of bubbles when the reducing agent is added in at 100 °C and no product is separable by centrifugation; for the later, triethylamine borane is sublimated on the cool part of glassware and no product can be

obtained. We also test KBH_4 and LiBH_4 ; no reaction has been found for KBH_4 , but the reaction is very fast for LiBH_4 and no product is separable by centrifugation. The hydride, with low melting point (LiBH_4 , 275 °C) or compatible with organic phase (TBAB), react too fast to form stable nuclei before the dissociation of $\text{Nd}(\text{acac})_3$ and $\text{Fe}(\text{acac})_3$. Triethylamine borane complex are stable at the reflux temperature of the solvent and surfactants for its three B-C covalent chemical bonds. This could be the reason why superhydride (LiBEt_3H) has been selected to synthesize colloidal ϵ -Co nanoparticles: to form homogenous solution in organic phase (Diocylether) and to avoid the possible incorporation of B atoms into ϵ -Co. In the series of LiBH_4 , NaBH_4 (m.p., 400 °C), and KBH_4 (m.p, 500 °C), only NaBH_4 can react steadily with the precursors and surfactants (OA and OM) in organic solution near 300 °C to form stable nuclei and its solid state ensures the following growth process. Thus, the suitable chemical reactivity of NaBH_4 and its solid state at the selected aging temperature realize the reasonable separation between nucleation and growth. When the temperature increases to 275 °C, there are small bubbles in the reaction, which are the bubbling effects taking place through absorbing local latent heat released from the exothermic reactions involved in the nucleation and growth of magnetic nanoparticles. The bubbling effects facilitate the formation of a huge number of nuclei.^[13] The reactions in the system is rather complex. At least, amidation reaction between OA and OM, the dissociation of $\text{Nd}(\text{acac})_3$ and $\text{Fe}(\text{acac})_3$ (facilitated by surfactants, such as OA and OM, and/or by hydride), and the reduction of $\text{Fe}(\text{III})$ by borohydride are involved.^[14] Because of the very high positive redox potential of metal Nd, NaBH_4 cannot reduce $\text{Nd}(\text{III})$ to Nd, supported by the XPS peak of Nd $3d_{5/2}$ at 982 eV, being the same value of Nd_2O_3 (see Supplementary Information, Figure S3). Even this reduction reaction occurs, the water molecules from the above-mentioned amidation reaction and OA can oxidize it to $\text{Nd}(\text{III})$. Considering the intrinsic oxophilic properties of $\text{Nd}(\text{III})$ and the presence of water and other oxygen-containing molecular species, the Nd-Fe-B-Na nanoparticles could contain some oxygen. These factors can contribute to the chemical stability to air, evaluated by the magnetic properties in the following part. These chemical reactions are different from the sputter deposition and melt spinning techniques on chemical composition control. We speculate that the reasons to form amorphous colloidal nanoparticles instead of crystalline ones are listed as follows. Firstly, the chemical potentials of the monomers (reactive atomic or molecular species) are usually high, and according to Ostwald's rule, the kinetically favoured metastable amorphous phase forms first.^[15] Secondly, the presence of $\text{Nd}(\text{III})$, sodium, some oxygen, and high content of boron could suppress the formation of crystalline phase. Thirdly, the temperature allowing us to synthesize ultrasmall and monodisperse nanoparticles (300-320 °C) is not high enough to rearrange and anneal the constituent atoms during growth. This rearrangement is usually associated with significant high thermal barriers.^[16] It is worth to note that it is likely a trend that ultrasmall nanoparticles adopt disordered structure compared to their bulk crystalline phases, such as chemically disordered face-centered cubic (fcc) for FePt colloidal nanocrystals,^[11] $(\gamma\text{-Fe}_2\text{O}_3)_{0.8}(\text{Fe}_3\text{O}_4)_{0.2}$ for Fe_3O_4 nanocrystals with diameter of 5 nm,¹⁰ and non-periodic and lack long-range atomic ordered structure of the Co and FeCo nanoparticles.^[17]

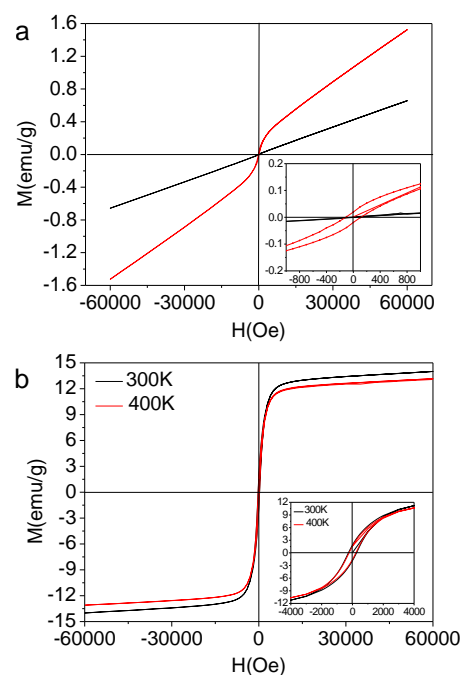


Figure 2 Magnetic properties of colloidal Nd-Fe-B-Na nanoparticles with different size. a, magnetic hysteresis of nanoparticle with 1 nm diameter (black curve) and 2 nm (red curve). b, magnetic hysteresis of nanoparticle with 3 nm diameter at 300 K (black curve) and 400 K (red curve).

The magnetic properties of the Nd-Fe-B-Na colloidal nanoparticles with size being 1 nm, 2 nm, and 3 nm corresponding to Figure 1 are measured with a SQUID-VSM system (MPMS, Quantum) in the temperature range lower than 400 K. The M-H magnetic hysteresis curves are depicted in Figure 2. The linear paramagnetic characterization is for the colloidal nanoparticle with 1 nm diameter. When the diameter increases to 2 nm, the ferromagnetic magnetic hysteresis loop is observed, with coercive field (H_c) being 120 Oe at 300 K (Figure 2a). The coercive field (H_c) of nanoparticles with 3 nm diameter is 262 Oe at 300K, 245 Oe at 400 K (Figure 2b). These H_c values are higher than that of bulk amorphous alloy measured at 300 K, about 10 Oe for $\text{Nd}_8\text{Fe}_{72}\text{B}_{20}$.^[12d] The saturation magnetization (M_s) at 6 T is 14 emu/g, comparable with that of Fe_3O_4 nanoparticles with the same size^[5c] which can exclude the possibility of the ferromagnetic properties originating from defect magnetism. In Figure 2, the time for the M-H measured at 400 K is twenty days later than the M-H curve measured at 300 K. From the M-H curve at 300 K in Figure 2b inset, we can see that the magnetic nanoparticles with 3 nm diameter cannot spontaneously magnetize or induced by the magnetic bar during colloidal synthesis. However, after the magnetic measurement at 300 K, the nanoparticle maintains its magnetic remanence at least for twenty days, as shown in Figure 2b inset for the M-H curve at 400 K. The stability in air of the Nd-Fe-B-Na colloidal nanoparticles is interrogated by the change of the magnetic properties after being exposed to air for two months. The coercive field (H_c) and magnetic remanence (M_r) decrease only by 0.5 percent, while the saturation magnetization (M_s) at 6 T decreases by 2.5 percent (see Supplementary Information, Figure S4). These indicate that the 3 nm nanoparticles are stable in air. The magnetic property decreasing after exposing to air several day are due to the oxidation of the trace surface unstable Fe (e.g., $\text{Fe}(\text{I})$ and $\text{Fe}(\text{II})$) or $\text{Fe}(\text{O})$ nanocluster.

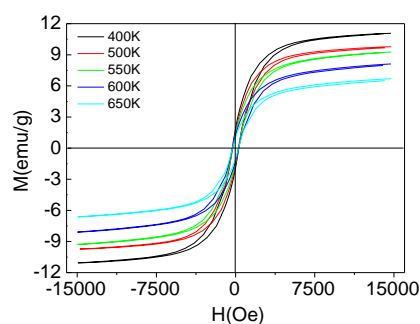


Figure 3 Magnetic properties of colloidal Nd-Fe-B-Na nanoparticles with 3 nm diameter at high temperature between 400 K and 650 K.

To shed more light on the structure and mag The magnetic properties of the 3 nm nanoparticle under temperature higher than 400 K are determined by LakeShore 7407 vibrating sample magnetometer (VSM) equipped with Hall probe. The M-H magnetic hysteresis curves and the magnetic parameters are given in Figure 3. As the temperature of the sample increases to 650 K, the saturation magnetization and magnetic remanence decrease. However, the coercive field (H_c) decreases some first and then increases a little, from 308 Oe to 270 Oe, and then to 293 Oe (see Supplementary Information, Figure S5). We do not measure the magnetic properties at the temperature higher than 650 K for the following considerations, higher temperature would decompose the organic surfactants (OA and OM) and result in the aggregation by annealing and sintering. The thermal analysis of the colloidal magnetic nanoparticles under nitrogen atmosphere is conducted (see Supplementary Information, Figure S6). There are an endothermic peak of DSC curve and a weight loss peak of TGA curve near 723 K, and these peaks can be tentatively assigned to the corresponding process of the decomposition of the organic surfactants of OA and OM and the fusion and aggregation of the nanoparticles. The magnetic properties at the temperature higher than 650 K would arise from the fusion and aggregation of the ‘naked’ nanoparticles, not at the single nanoparticle level. When the size increases to 5 nm (Figure 1d), the magnetic nanoparticles can spontaneously magnetize or induced by the magnetic bar during colloidal synthesis, shown in Figure S7. The coercive field (H_c) and magnetic remanence (M_r) are 612 Oe and 11.2 emu/g measured by LakeShore 7407 VSM at 300 K, while the saturation magnetization (M_s) at 1.8 T is 29.6 emu/g.

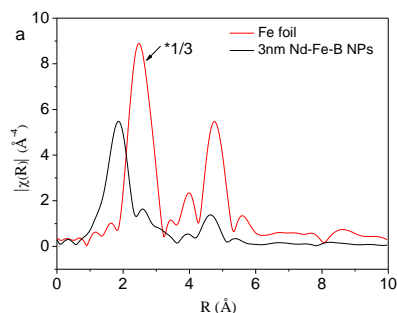


Figure 4 RDF's of the 3-nm Nd-Fe-B-Na nanoparticles and standard Fe foil.

Magnetic properties of the 3 nm Nd-Fe-B-Na nanoparticle, we perform Extended X-ray absorption fine structure (EXAFS) and Mössbauer spectroscopy characterization. The radial distribution functions (RDF) of the 3 nm Nd-Fe-B-Na nanoparticle and Fe foil,

obtained from their $k^3\chi(k)$ by Fourier transform in Figure S8, are depicted in Figure 4. There are several distinct peaks of the sample. Compare with the peaks of Fe foil, the peaks at 2.58 Å, 3.9 Å, and 4.6 Å of the sample can partially result from to the Fe⁰ nanocluster. The peak at 1.86 Å can be assigned to the amorphous phase. Structure parameters obtained by fitting the Fe K-edge data shown in Figure 4 are listed in Table S1. There are about 3.5 boron atoms and 1.2 Fe atoms around each Fe center. The nearest Fe-B and Fe-Fe distances are 1.99 Å and 2.91 Å. There are EXAFS characterizations on Nd₂Fe₁₄B nanomagnets and nanocomposites, but they are of crystalline and short of the fitted results of Fe-B and Fe-Fe chemical bonds. It's difficult to directly compare the crystalline phase with amorphous phase. The distance of Fe-B is shorter, while the distance of Fe-Fe is larger than those of the amorphous Fe-Si-B alloy, 2.27 Å and 2.54 Å, respectively.^[11b] The first peak in the RDF of the 3 nm nanoparticle is in slightly higher position than those of standard Fe₂O₃ and Fe₃O₄ in Figure S9, indicating the Fe-B bonds being slightly larger than the Fe-O chemical bonds.

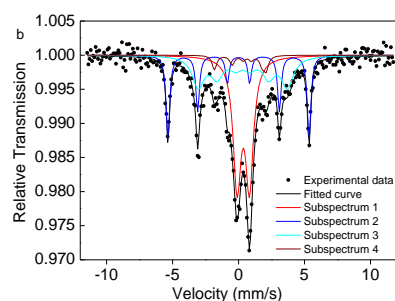


Figure 5 ⁵⁷Fe Mössbauer spectrum of the 3-nm Nd-Fe-B-Na nanoparticles measured at 300 K.

⁵⁷Fe Mössbauer spectroscopy of the sample measured at 300 K in Figure 5 and Table S2 confirms that there is a sextet subspectrum of subarea of 24 % (Subspectrum 2) with the same isomer shift (δ) as that of Fe foil and a hyperfine field of 33.3 kOe attributed to unoxidized Fe⁰ nanoparticles in a blocked state, assigned to Fe⁰ nanocluster(s).^[18] To exclude the possibility of the sextet subspectrum resulting from very large Fe nanoparticles not observed by TEM, we characterize the dynamic light scattering (DLS) of the 3 nm Nd-Fe-B-Na nanoparticles dispersed in hexane, there is no signal of particles with hydrodynamic diameter larger than 7 nm (Figure S10). For freestanding colloidal Fe nanoparticle, the blocking temperature of unoxidized 4.5 nm Fe nanoparticles is just 110 K.^[19] We speculate that the sextet subspectrum of the Fe⁰ nanocluster(s) could originate from their exchange-coupling with the amorphous parts surrounding them inside the 3 nm Nd-Fe-B-Na nanoparticle. This structure feature is in accordance with the RDF of the nanoparticles in Figure 4. Although the temperature to measure Mössbauer effect is far below T_C , there is still a doublet peak with 40 % subarea. This phenomenon is different from the magnetic behavior of CoFe₂O₄ nanocrystals and Fe nanocube assembly with only one sextet peak under the blocking temperature, probably due to structure disorder and surface effect.^[4a,18] Because of the surface effect and complex chemical composition, the Mössbauer spectra are also different from those of bulk amorphous Fe-B-Si, the bulk without any doublet peak.^[11b] However, there is no signal of Fe⁰ nanocluster in the 5 nm nanoparticles shown in Figure S11 and

Table S3, probably due to higher synthetic temperature being able to destroy the Fe nanocluster by forming Fe-B chemical bonds. As the size increases to 5 nm, the subarea of the doublet peak from Fe nuclei with unblocked state decreases slightly to 37 %. For the nanoparticles with 1 nm or 2 nm, there are only two doublet peaks, although the H_c is 120 Oe of the 2 nm one (Figure S11 and Table S3).

For the present colloidal Nd-Fe-B-Na nanoparticles, when the size decreases to 1 nm, the zero-field-cooling (ZFC) magnetization (Figure S12) under 1000 Oe magnetic field indicates that there is no peak magnetization between 2 K and 305 K, unlike those of ϵ -Co, CoFe_2O_4 , and Fe_3O_4 magnetic nanoparticles.^[1,4a,5a] These results probably arise from finite size effects suppressing the magnetic ordering. Considering the ferromagnetic properties of the magnetic nanoparticles larger than 2 nm (Figure 2a, red curve), the size is the crucial factor to determine the magnetic exchange model. The critical size of the present colloidal Nd-Fe-B-Na nanoparticle from the experimental results should be between 1 nm and 2 nm, which is close to the estimated grain size of Gd-Co amorphous films (smaller than 25 Å) and the diameter of Fe-enriched clusters simulated in the inhomogeneous $\text{Fe}_{67}\text{Y}_{33}$ alloys (about 15–20 Å).^[10a,11a]

Conclusions

In summary, the controlled colloidal synthesis of amorphous Nd-Fe-B-Na nanoparticles and the size dependence of the magnetic properties have been demonstrated in sub-5-nm regime. The magnetic nanoparticle with 3 nm diameter exhibit ferromagnetic magnetic properties even at temperature as high as 650 K. The structure of the 3 nm Nd-Fe-B-Na nanoparticles has been characterized by EXAFS and Mössbauer spectroscopy. These characteristics clearly demonstrate that such Nd-Fe-B-Na nanoparticles present opportunities for fundamental studies of nanomagnetism, as well as for potential ultrahigh density magnetic recording, permanent magnetic nanocomposites, catalysis, and biological applications. The present colloidal method can also be used to grow colloidal nanoparticles of other amorphous metal alloys with nanometer size, with potential importance in magnetic, magneto-optic, and electronic applications.

Acknowledgements

This work is supported by the National Natural Science Foundation of China (91122003) and Developing Science Funds of Tongji University.

Notes and references

^a Department of Chemistry, Tongji University, Shanghai 200092, P. R. China. Fax: (+86) 21-65982287; E-mail: byan@tongji.edu.cn; b

^b Shanghai Synchrotron Radiation Facility, Shanghai Institute of Applied Physics, Chinese Academy of Sciences, Shanghai 201204, China

† Electronic Supplementary Information (ESI) available: [details of any supplementary information available should be included here]. See DOI: 10.1039/c000000x/

- 1 S. H. Sun, C. B. Murray, D. Weller, L. Folks and A. Moser, *Science*, 2000, **287**, 1989.
- 2 (a) S. H. Sun and C. B. Murray, *J. Appl. Phys.*, 1999, **85**, 4325; (b) C. T. Black, C. B. Murray, R. L. Sandstrom and S. H. Sun, *Science*, 2000, **290**, 1131; (c) V. F. Puentes, K. M. Krishnan and A. P. Alivisatos, *Science*, 2001, **291**, 2115.
- 3 H. Zeng, J. Li, J. P. Liu, Z. L. Wang and S. H. Sun, *Nature*, 2002, **420**, 395.
- 4 (a) C. Liu, B. S. Zou, A. J. Rondinone and J. Zhang, *J. Am. Chem. Soc.*, 2000, **122**, 6263; (b) T. Hyeon, S. S. Lee, J. Park, Y. Chung and H. Bin Na, *J. Am.*

- Chem. Soc.*, 2001, **123**, 12798; (c) J. I. Park and J. Cheon, *J. Am. Chem. Soc.*, 2001, **123**, 5743; (d) S. H. Sun and H. Zeng, *J. Am. Chem. Soc.*, 2002, **124**, 8204.
- 5 (a) J. Park, K. J. An, Y. S. Hwang, J. G. Park, H. J. Noh, J. Y. Kim, J. H. Park, N. M. Hwang and T. Hyeon, *Nat. Mater.*, 2004, **3**, 891; (b) J. Park, E. Lee, N. M. Hwang, M. S. Kang, S. C. Kim, Y. Hwang, J. G. Park, H. J. Noh, J. Y. Kim, J. H. Park and T. Hyeon, *Angew. Chem., Int. Ed.*, 2005, **44**, 2872; (c) B. H. Kim, N. Lee, K. An, Y. I. Park, Y. Choi, K. Shin, Y. Lee, S. G. Kwon, H. B. Na, J. G. Park, T. Y. Ahn, Y. W. Kim, W. K. Moon, S. H. Choi and T. Hyeon, *J. Am. Chem. Soc.*, 2011, **133**, 12624; (d) J. Dobson, *Nat. Nanotechnol.*, 2008, **3**, 139.
- 6 (a) C. Tassa, S. Y. Shaw and R. Weissleder, *Acc. Chem. Res.*, 2011, **44**, 842; (b) D. Yoo, J. H. Lee, T. H. Shin and J. Cheon, *Acc. Chem. Res.*, 2011, **44**, 863; (c) D. Ho, X. L. Sun and S. H. Sun, *Acc. Chem. Res.*, 2011, **44**, 875; (d) J. H. Lee, J. T. Jang, J. S. Choi, S. H. Moon, S. H. Noh, J. W. Kim, J. G. Kim, I. S. Kim, K. I. Park and J. Cheon, *Nat. Nanotechnol.*, 2011, **6**, 418.
- 7 (a) A. H. Lu, W. Schmidt, N. Matoussevitch, H. Bonnemann, B. Spliethoff, B. Tesche, E. Bill, W. Kiefer and F. Schuth, *Angew. Chem.*, 2004, **43**, 4303; (b) M. Shokouhimehr, Y. Z. Piao, J. Kim, Y. J. Jang and T. Hyeon, *Angew. Chem., Int. Ed.*, 2007, **46**, 7039; (c) V. Mazumder, M. F. Chi, K. L. More and S. H. Sun, *J. Am. Chem. Soc.*, 2010, **132**, 7848; (d) Y. M. Lee, M. A. Garcia, N. A. F. Huls and S. H. Sun, *Angew. Chem. Int. Ed.*, 2010, **49**, 1271; (e) S. J. Guo, S. Zhang, X. L. Sun and S. H. Sun, *J. Am. Chem. Soc.*, 2011, **133**, 15354.
- 8 (a) J. P. Ge, Y. X. Hu and Y. D. Yin, *Angew. Chem., Int. Ed.*, 2007, **46**, 7428; (b) J. P. Ge, L. He, J. Goebel and Y. D. Yin, *J. Am. Chem. Soc.*, 2009, **131**, 3484; (c) J. P. Ge and Y. D. Yin, *Angew. Chem. Int. Ed.*, 2011, **50**, 1492; (d) Y. X. Hu, L. He and Y. D. Yin, *Angew. Chem., Int. Ed.*, 2011, **50**, 3747.
- 9 (a) N. G. Akdogan, W. F. Li and G. C. Hadjipanayis, *J. Appl. Phys.*, 2011, **109**, 07A759; (b) C. W. Kim, Y. H. Kim, U. Pal and Y. S. Kang, *J. Mater. Chem. C*, 2013, **1**, 275; (c) A. Hussain, A. P. Jadhav, Y. K. Baek, H. J. Choi, J. Lee and Y. S. Kang, *J. Nanosci. Nanotechnol.*, 2013, **13**, 7717.
- 10 (a) P. Chaudhari, J. J. Cuomo and R. J. Gambino, *Appl. Phys. Lett.*, 1973, **22**, 337; (b) Y. Togami, *Appl. Phys. Lett.*, 1978, **32**, 673; (c) R. Harris, M. Plischke and M. J. Zuckermann, *Phys. Rev. Lett.*, 1973, **31**, 160.
- 11 (a) D. Spisak, J. Hafner and R. Lorenz, *J. Magn. Magn. Mater.*, 1997, **166**, 303; (b) Y. Takahara and N. Narita, *Mat. Sci. Eng. A*, 2001, **315**, 153; (c) N. Hassanain, H. Lassri, R. Krishnan and A. Berrada, *J. Magn. Magn. Mater.*, 1995, **146**, 37; (d) N. Hassanain, H. Lassri, R. Krishnan and A. Berrada, *J. Magn. Magn. Mater.*, 1995, **146**, 315.
- 12 (a) M. Slimani, M. Hamedoun, H. Lassri, S. Sayouri and R. Krishnan, *J. Magn. Magn. Mater.*, 1996, **153**, 132; (b) M. Slimani, M. Hamdoun, M. Tlemcani, H. Arhouchi and S. Sayouri, *Physica B*, 1997, **240**, 372; (c) E. H. Sayouty, F. Annouar, H. Lassri, N. Randrianantoandro and J. M. Greneche, *J. Alloys Compds.*, 2005, **397**, 47; (d) N. Hassanain, H. Lassri, A. Berrada and R. Krishnan, *Phys. Stat. Sol. C*, 2006, **3**, 3239.
- 13 J. Lynch, J. Q. Zhuang, T. Wang, D. LaMontagne, H. M. Wu and Y. C. Cao, *J. Am. Chem. Soc.*, 2011, **133**, 12664.
- 14 (a) N. R. Jana, Y. F. Chen and X. G. Peng, *Chem. Mater.*, 2004, **16**, 3931; (b) J. Joo, S. G. Kwon, J. H. Yu and T. Hyeon, *Adv. Mater.*, 2005, **17**, 1873; (c) H. M. Wu, Y. G. Yang and Y. C. Cao, *J. Am. Chem. Soc.*, 2006, **128**, 16522; (d) H. T. Zhang, D. H. Ha, R. Hovden, L. F. Kourkoutis and R. D. Robinson, *Nano Lett.*, 2011, **11**, 188; (e) Q. Zhang, B. Yan, F. Lei and H. H. Chen, *Nanoscale* 2012, **4**, 7646.
- 15 W. Z. Ostwald, *Phys. Chem.*, 1897, **22**, 289.
- 16 L. E. M. Howard, H. L. Nguyen, S. R. Giblin, B. K. Tanner, I. Terry, A. K. Hughes and J. S. O. Evans, *J. Am. Chem. Soc.*, 2005, **127**, 10140.
- 17 (a) D. P. Dinega and M. G. Bawendi, *Angew. Chem., Int. Ed.*, 1999, **38**, 1788; (b) B. Chaudret, C. Desvieux, C. Amiens, P. Fejes, P. Renaud, M. Respaud, P. Lecante and E. Snoeck, *Nat. Mater.*, 2005, **4**, 750.
- 18 F. Dumestre, B. Chaudret, C. Amiens, P. Renaud and P. Fejes, *Science*, 2004, **303**, 821.
- 19 T. C. Monson, E. L. Venturini, V. Petkov, Y. Ren, J. M. Lavin and D. L. Huber, *J. Magn. Magn. Mater.*, 2013, **331**, 156.